

# Active inference as a unified model of collision avoidance behavior in human drivers

Julian F. Schumann<sup>1</sup>, Johan Engström<sup>2\*</sup>, Leif Johnson<sup>2</sup>, Matthew O’Kelly<sup>2</sup>,  
Joao Messias<sup>2</sup>, Jens Kober<sup>1</sup>, Arkady Zgonnikov<sup>1</sup>

<sup>1</sup>Department of Cognitive Robotics, Delft University of Technology, Netherlands.

<sup>2</sup>Waymo LLC, Mountain View, CA, USA.

Contributing authors: [j.f.schumann@tudelft.nl](mailto:j.f.schumann@tudelft.nl); [jengstrom@waymo.com](mailto:jengstrom@waymo.com); [leif@waymo.com](mailto:leif@waymo.com);  
[mokelly@waymo.com](mailto:mokelly@waymo.com); [jmessias@waymo.com](mailto:jmessias@waymo.com); [j.kober@tudelft.nl](mailto:j.kober@tudelft.nl); [a.zgonnikov@tudelft.nl](mailto:a.zgonnikov@tudelft.nl);

## Abstract

Collision avoidance – involving a rapid threat detection and quick execution of the appropriate evasive maneuver – is a critical aspect of driving. However, existing models of human collision avoidance behavior are fragmented, focusing on specific scenarios or only describing certain aspects of the avoidance behavior, such as response times. This paper addresses these gaps by proposing a novel computational cognitive model of human collision avoidance behavior based on active inference. Active inference provides a unified approach to modeling human behavior: the minimization of free energy. Building on prior active inference work, our model incorporates established cognitive mechanisms such as evidence accumulation to simulate human responses in two distinct collision avoidance scenarios: front-to-rear lead vehicle braking and lateral incursion by an oncoming vehicle. We demonstrate that our model explains a wide range of previous empirical findings on human collision avoidance behavior. Specifically, the model closely reproduces both aggregate results from meta-analyses previously reported in the literature and detailed, scenario-specific effects observed in a recent driving simulator study, including response timing, maneuver selection, and execution. Our results highlight the potential of active inference as a unified framework for understanding and modeling human behavior in complex real-life driving tasks.

Collision avoidance is a critical skill for human drivers. It involves the rapid detection of threats (such as a vehicle ahead suddenly braking) and deciding on an appropriate evasive maneuver (for instance, braking or swerving). These maneuvers are complex, requiring not only precise execution but also continuous adjustments as the situation evolves. Furthermore, drivers need to account for the uncertainty in the future behavior of other road users: for example, will an oncoming vehicle encroaching into my lane continue across or move back to its own lane? Understanding how humans

avoid collisions in traffic can provide insights into high-stakes, split-second decision making which has substantial implications for traffic safety.

Behavior models play a key role both in understanding the mechanisms of human collision avoidance and in improving traffic safety. These models are applied in diverse contexts, such as collision risk estimation [1], understanding effects of driver distraction [2], modeling take-over behavior [3], representing human agents in simulated test environments [4], and providing behavioral benchmarks for autonomous vehicles [5, 6].

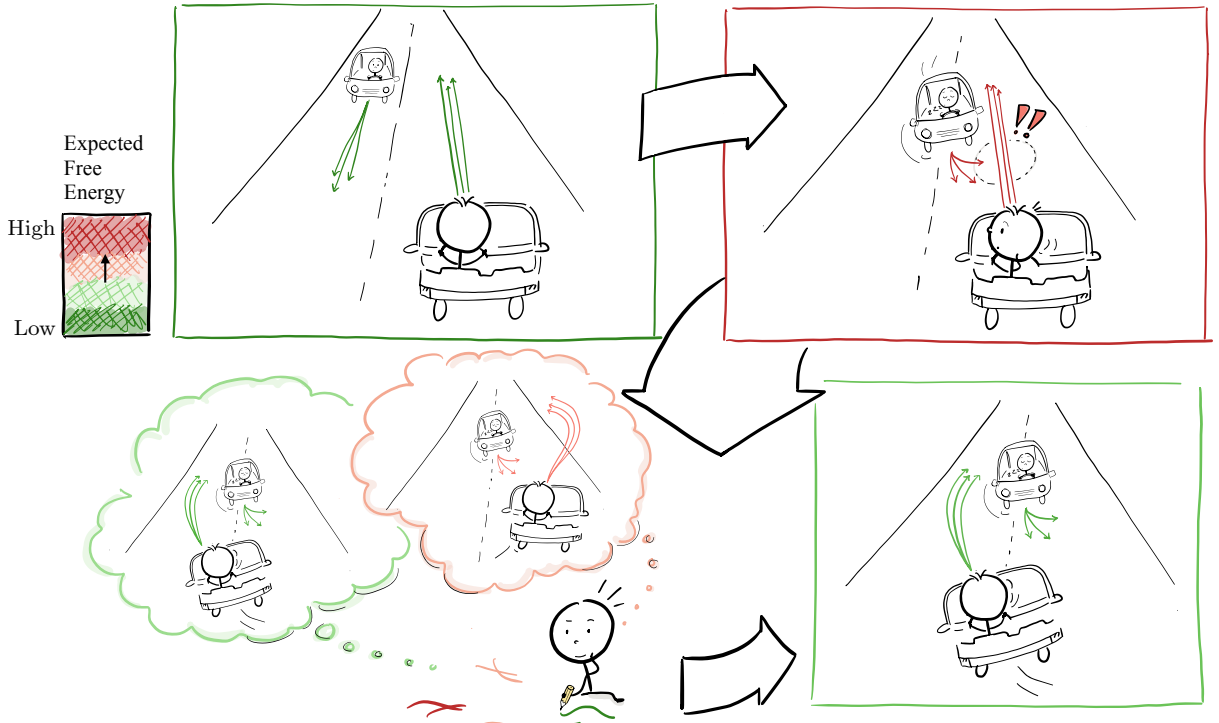


**Fig. 1:** An illustration of the key principles of our active inference model in the opposite-direction lateral incursion scenario. Upper left panel: The modeled agent (at the bottom, facing forward) is continuously generating beliefs (represented by the arrows) about how the current driving situation will play out and what future observations it will make as a consequence of its own actions and the actions of the other vehicle. In "normal", non-conflict situations, the situation typically plays out as expected. The agent thus initially believes with high certainty that both itself and the oncoming vehicle will remain in their lanes and pass each other safely. This yields low expected free energy (EFE; green arrows) since the agent's expected (and thus preferred) observations (e.g., making progress, avoid collisions) are aligned with the actual observations. Upper right panel: When the oncoming vehicle suddenly encroaches into the driver's lane, the EFE increases rapidly (as indicated by the red arrows) because this new situation is likely to result in an observed collision in the future, which is strongly disfavored by the agent. In this situation, the agent's belief about the oncoming vehicle's future trajectory also becomes more uncertain, because the other vehicle can no longer be trusted to follow established traffic norms. The agent thus needs to imagine a better future with lower EFE – in this case, a scenario where it avoids collision by swerving left (lower left panel) and take action to make that better future come true (lower right panel).

Besides immediate practical applications, modeling human collision avoidance behavior is an interesting subject of study in its own right. Being a highly complex and dynamic task with extremely high stakes, collision avoidance provides a unique testbed for theories and models of cognition previously not validated in the real world [7–9].

Most existing computational models of human collision avoidance are mechanistic, that is, are

based on the explicit modeling of cognitive mechanisms underlying response timing and evasive maneuvering. However, they are typically fragmented, focusing either on specific scenario types (e.g., front-to-rear conflicts [10–12] or merging [13]), specific explanatory factors (such as off-road glances [1, 14] or cognitive load [2]), or only reproduce certain aspects of human behavior (such as response times [3, 6, 10, 11, 15] or

the extent of steering [16]). Altogether, these models cover a wide range of scenarios and diverse aspects of collision avoidance behavior. Yet, each one of these mechanistic models on its own is highly specific: they are not designed to generalize to multiple scenarios or describe multiple aspects of human behavior.

Recently, machine learning models based on large datasets of human driving have demonstrated the ability to generalize across a wide range of traffic scenarios [4, 17–21]. Because such models typically generate full motion trajectories, they also have the potential to represent multiple aspects of collision avoidance behavior and not just a single metric of interest. However, a key challenge is that safety-critical behavior such as collision avoidance is often under-represented in the datasets used for training [22], which makes it hard to achieve representative human-like collision avoidance behavior solely based on learning from data [23].

Thus, there is currently a lack of models that can capture the key aspects of human collision avoidance behavior (response selection, timing, and execution) all at the same time and across different scenarios. This limits both practical applications (due to the need to develop a new model for every new scenario) and fundamental understanding of cognitive mechanisms underlying the behavior of humans in safety-critical situations in traffic (due to the lack of a unified explanation for multiple aspects of behavior).

To address this gap, here we present a unified collision avoidance model based on active inference. Originating in computational neuroscience, active inference is a versatile general framework for understanding and modeling sentient behavior in living systems [24–26] that has been previously used to model human behavior in diverse contexts [27–31], including the modeling of human driver behavior such as car following [32], responses to driving automation failures [15], and managing uncertainty around occlusions and non-driving-related tasks [33]. Building on the model of Engström *et al.* [33], here we propose an active inference-based model to capture a spectrum of human behaviors in collision avoidance. Our model incorporates several well-known cognitive mechanisms to represent the dynamics of human decision making in response to sudden stimuli,

such as looming perception [34, 35] and evidence accumulation [36–39]. We evaluated our model against a range of previously reported empirical findings in two paradigmatic collision avoidance scenarios: the front-to-rear scenario, where a driver needs to respond to a suddenly braking vehicle in front, and the opposite-direction lateral incursion scenario, where an oncoming vehicle suddenly cuts across the driver’s path. Testing the model in two markedly different scenarios allowed us to investigate the potential of active inference as a unified framework for generalizable modeling of human collision avoidance behavior.

## Results

In this work, we use active inference as an overarching framework to guide the modeling. The key premise of active inference is that all behavior and cognition can be understood based on the single principle of minimizing *free energy*. An agent minimizing free energy can be conceptually understood as the agent sensing, and acting upon, the world in such a way as to minimize its surprise over time. In the active inference framework, this amounts to seeking out observations that are *expected* (unsurprising) and preferred given the type of creature the agent is, reflecting its adaptation to its particular environment or niche (e.g., a fish expects and prefers the sensation of being immersed in water). Agents capable of planning into the future and modeling the consequences of their actions (such as human car drivers), select plans that minimize the *expected surprise*, or more generally the *expected free energy* (EFE) [24].

Our model implements these principles in the collision avoidance context (Figure 1). Specifically, the modeled agent repeatedly evaluates possible futures under its current policy (i.e., a sequence of planned actions) – including interactions with other road users – in terms of their EFE. The driver then selects policies that minimize EFE by realizing observations that align with the driver’s preferences such as avoiding collisions (yielding *pragmatic value*) while obtaining new information to reduce uncertainty about the environment’s future (yielding *epistemic value*) [24, 33].

Fundamentally, agents cannot have perfect knowledge of the mechanisms underlying the surrounding world (the *generative process*), but

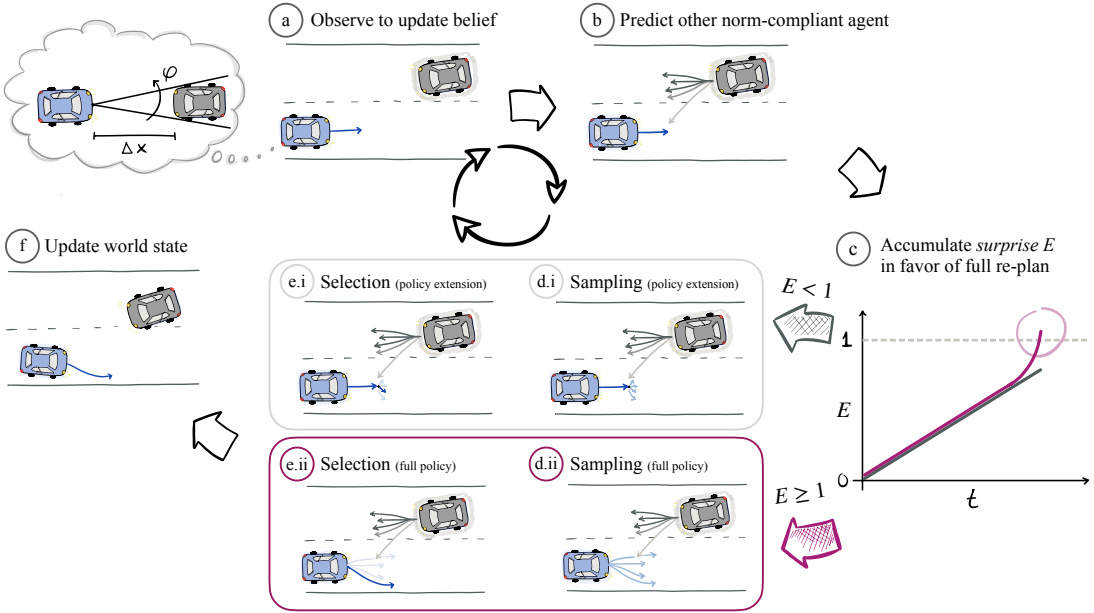


**Fig. 2:** Main functional components of our active inference collision avoidance model. At each time step, the ego agent observes the world state, updates its belief about the world (a), and makes probabilistic predictions about the actions of the other agent (where future trajectories that adhere to traffic norms are prioritized) (b). At every time step, the agent accumulates evidence (as measured by surprise associated with the current state of the world) on the unsuitability of the current policy (c). If the accumulated evidence reaches a threshold, the agent re-plans the entire policy, selecting the one that minimizes the expected free energy (EFE) (d.ii and e.ii). Otherwise, it continues using its current policy in an extend form – i.e., only sampling and then selecting the policy’s last time step (d.i and e.i). The first action in the new or extended policy is then applied to the environment (f).

instead rely on an internal, not necessarily veridical, representation of their beliefs about the environment, the *generative model* [24]. Importantly, an (*ego*) agent’s *generative model* is probabilistic, with the uncertainty about the state of the world being represented by a set of sample particles. Our model implements these general principles in a time-discrete, sequential process (Figure 2) which incorporates a number of key perceptual, cognitive, and motor mechanisms.

**Looming-based perception.** First, the agent observes the world and updates its belief (Figure 2a), combining these observations with the expectations derived from the generative model propagating its previous belief forward in time. The model assumes that the agent cannot directly perceive kinematic states of surrounding objects (e.g., positions and velocities), but instead uses

the readily available perceptual information [35]: the object’s visual angle  $\varphi$  subtended at the driver’s retina, and its derivative, the angular rate  $\dot{\varphi}$ , commonly referred to as *looming* [34, 40? ]. The model then infers back the kinematic state from those observations, where – with increasing distances – equal variations in  $\varphi$  lead to increasingly larger variations in the inferred distance and therefore increasing uncertainty about the kinematic state of the other agent. Additionally, the agent’s perception accuracy is limited: it cannot perceive looming with absolute values below a threshold  $\dot{\varphi}_0$  [41, 42]. Due to this threshold, the agent is unable to detect small relative velocities at long distances; our model thus incorporates this looming threshold as one possible mechanism behind delays in recognizing events like abrupt braking of the other vehicle.

**Behavior prediction via norm-conditioned particle filter.** After perceiving the environment, the ego agent predicts the other vehicle’s behavior (Figure 2b). For this, our model uses a sample-based approach [33, 43] (i.e., based on a particle filter). Specifically, the samples representing the agent’s updated belief about the other vehicle are propagated forward by the *generative model* (in our case using a bicycle model with additive Gaussian noise). In this way, the model generates multiple distinct kinematically plausible future trajectories of the other vehicle, including the ones that could potentially lead to a collision. This enables the model to anticipate rare, long-tail behaviors of the other vehicle and respond to them appropriately during collision avoidance, but yields overly pessimistic predictions in non-conflict situations. For instance, widely dispersed predictions could lead the agent to anticipate vehicles encroaching into its lane, incentivizing unnecessary evasive actions. By contrast, human drivers typically assume that other vehicles follow traffic rules [44, 45] and other societal norms for driving [46]. To capture this, our model assumes that the ego agent uses a *norm-conditioned particle filter* for behavior prediction, by assigning each possible predicted trajectory a weight based on its adherence to traffic norms. This allows the model to prioritize norm-compliant behaviors when predicting the actions of the other vehicle. In this way, the model’s belief about the future trajectory of the other vehicle is initially constrained by the social norm that other vehicles typically remain within their lane unless explicitly indicating otherwise. However, when another vehicle unexpectedly initiates a conflict (for example an incursion towards the ego vehicle’s lane), the model will eventually take predicted norm-violating trajectories seriously. The reason for this is that the weights assigned to each predicted particle in the set are divided by their sum (i.e., sum to 1 across all predictions). Thus, in cases where the overwhelming majority of the predicted trajectories violate the norms, the model still considers these trajectories rather than disregarding all of them as non-norm-compliant.

**Re-planning full policy based on accumulating surprise.** In the next step, based on the set of previously predicted possible trajectories of the other vehicle, the agent considers its

own policy, evaluating its current suitability by calculating the *residual information* [47] of the *pragmatic value*, which can be seen as a measure of *surprise*. This surprise signal – the (scaled) negative pragmatic value associated with the currently selected policy – essentially indicates how unsuitable the current policy is given the model’s preferred observations and how the situation is expected to develop. The model assumes that the driver continuously accumulates this surprise signal as evidence in favor of full policy re-plan (Figure 2c). On each time step, if the accumulated evidence has not reached a predefined threshold, the agent considers it sufficient to continue with the current policy, and extends this policy one time step into the future (Figure 2d.i and e.i). However, if enough evidence in favor of current policy being unsuitable is accumulated, a set of completely new policies is sampled and a new full policy is selected (Figure 2d.ii and e.ii). The first action from either the extended or the new full policy is then applied to update the environment for the next time step (Figure 2f).

**Constrained policy sampling.** When proposing new candidate policies, either for extension (Figure 2d.i) or full re-plan (Figure 2d.ii), the model uses the *cross-entropy method* [48]. With this method, candidate actions are iteratively resampled, increasingly focusing on the most promising areas of the action space. To represent humans’ bounded capacity for planning under time pressure [13, 49–52], we limit the number of evaluated policies in this process. Importantly, the sampled acceleration values are constrained to reflect that humans operate the gas and brake pedals with one foot. These constraints include limiting applied jerks (as humans cannot press or release pedals instantaneously) and enforcing a constant holding time of 0.2 s at acceleration  $a_0 \lesssim 0 \text{ ms}^{-2}$  during transitions in both directions between acceleration and deceleration (as humans cannot move their foot between pedals instantaneously).

**Policy selection via expected free energy minimization.** Among the sampled candidate policies, the model aims to find the policy that minimizes *expected free energy* (EFE) – the cornerstone of the active inference framework (Figure 2e.i and e.ii). In our model, the pragmatic

value part of the EFE is maximized by 1) maintaining a desired longitudinal velocity, 2) staying within the current lane (avoiding unnecessary or unsafe lane changes) and on the road, 3) minimizing control inputs (avoid harsh braking or steering), 4) preventing collisions or at least reducing their severity (measured by the relative impact velocity), and 5) avoiding situations where collisions may become inevitable (such as following a vehicle too closely without sufficient stopping distance, assuming realistic reaction times). Finally, maximizing the epistemic value encourages 6) policies resulting in a large variety of reliable observations [33]. However, in the present collision avoidance setting, behavior is mainly expected to be driven by pragmatic, rather than epistemic, value since there is not much the driver can do to reduce uncertainty, especially given that we here assume that the other vehicle is non-reactive to the ego agent's actions.

## Model evaluation

We evaluated the model against human data in two scenarios. In the *front-to-rear* scenario, we compared the model to the results of a meta-analysis of brake response times [53] in experimental driving simulator and field studies (e.g., Brookhuis *et al.* [54] and Lee *et al.* [55]), and an analysis of deceleration magnitudes based on two naturalistic driving datasets captured across US and Africa reported in [14]. In the *opposite-direction lateral incursion* scenario, the model was compared to human data from a driving simulator study conducted in UK [56] which was conducted in parallel to the present work. Thus, by contrast to the model evaluation for the front-to-rear scenario, which was based on aggregated data, we were here able to run our model on nearly identical scenarios for which the human data was collected, allowing for more detailed comparisons. Importantly, the same model parameter values were used for both scenarios.

### Front-to-rear scenario

In the front-to-rear scenario, the ego vehicle trails the other vehicle which is driving in the same lane; both vehicles have the same initial velocity which was systematically varied in our simulations together with the initial time gap between

the vehicles. After a short time of driving at constant speed, the other vehicle starts braking with a high constant deceleration until coming to a stop. Depending on the initial kinematics of the vehicles, the ego agent can avoid collision either solely by braking (Figure 3a) or combined braking and swerving (Figure 3b). The model sometimes avoided a collision by swerving only (i.e., without braking). However, since existing results in the literature on front-to-rear scenarios typically only report on braking response performance, we only compared our models brake response times (i.e., for the analysis of those, steering only responses are not considered).

At lower speeds and larger time gaps, the model typically avoids collisions by braking only. In a representative simulation (Figure 3a), after the leading agent started braking at  $t = 0.8$  s (first dashed line), it took the model 0.6 s to perceive this (see the ego agent's belief in the acceleration plot). At that point ( $t = 1.4$  s, second dashed line), the model recognized the imminent conflict resulting from this change in perceived behavior of the other vehicle, as can be seen by the rapid decrease (increase in negative value) in the collision part of the pragmatic value. This leads to a corresponding increase in the rate of accumulation of the evidence for a re-plan (i.e., surprise). However, it still took further 0.6 s until the accumulated evidence  $E$  reached the threshold, delaying the first noticeable agent reaction to  $t = 2$  s (third dashed line), where the agent started to execute a new policy – emergency braking. This policy was selected because it allowed the agent to drastically reduce its EFE via reaching future states with high pragmatic value, in particular thanks to low collision probability. This policy was preferred over the alternative policy of braking and steering into the adjacent lane because the pragmatic value associated with lane changing was more negative than that associated with lower velocity, as the desired (corresponding to the initial) velocity is comparatively low. However, even under this policy, at  $t = 2$  s, the acceleration has still not changed, due to the pedal constraints. Consequently, the first deceleration of the model can be observed at  $t = 2.2$  s, resulting in a total response time of 1.4 s.

Smaller time gaps and higher initial velocities can make it kinematically impossible to avoid collision by braking only. In such situations, the model typically opts to steer and brake at the

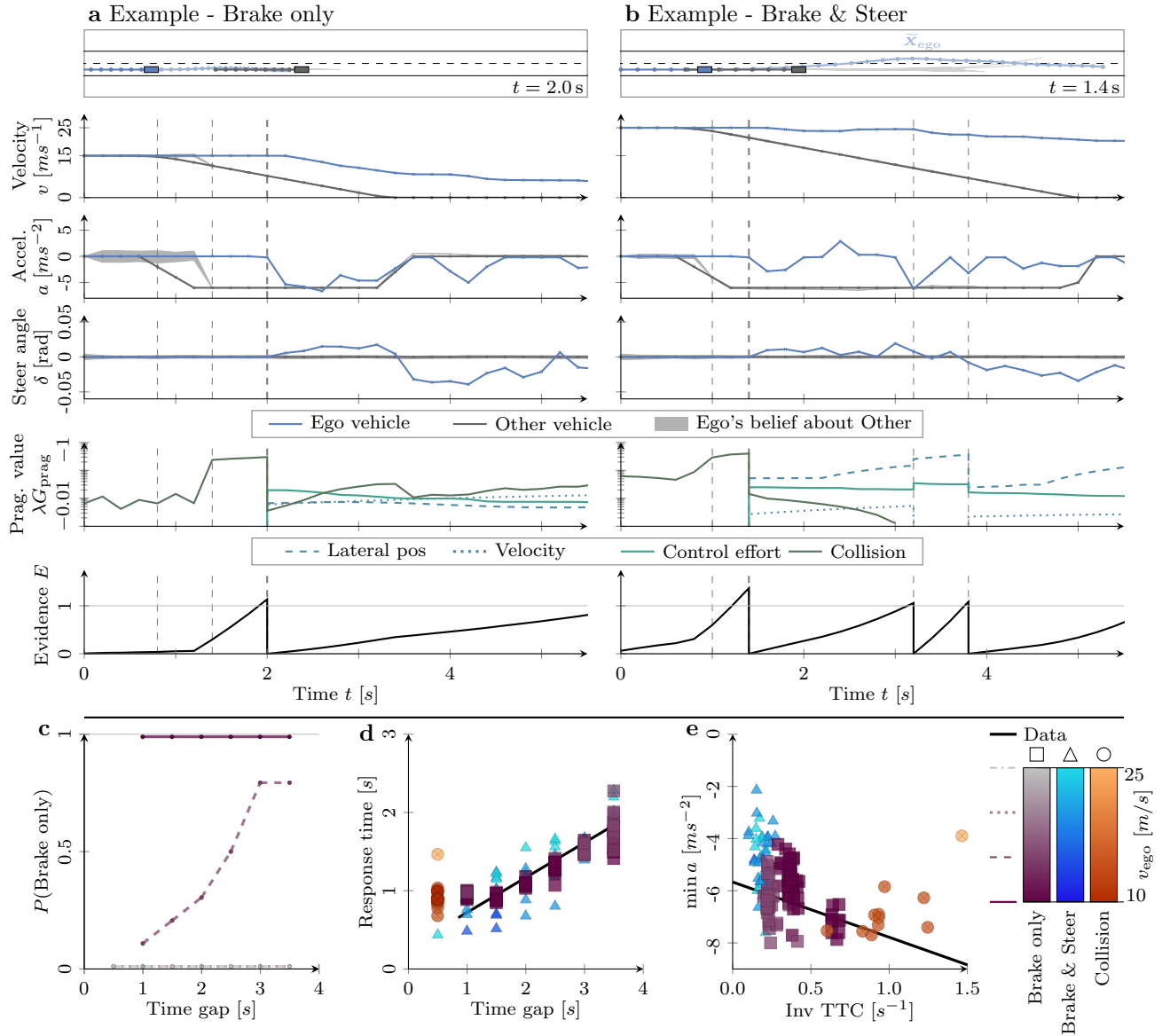


**Fig. 3:** Evaluation of the model in the front-to-rear scenario. **a)** In a scenario where initial pre-conflict kinematics are such that collision can be avoided by braking (initial vehicle velocities  $v_0 = 15 \text{ ms}^{-1}$ , a bumper-to-bumper time gap of 1.5 s), the model typically produces braking-only behavior. The sub-panels visualize the top-down view of the scenario, the time dynamics of both vehicles' velocity  $v$ , acceleration  $a$ , steering angle  $\delta$  and (for the ego vehicle) the components of the pragmatic value  $G_{\text{prag}}$  (scaled with the evidence accumulation gain  $\lambda$ ) that underlie the accumulated evidence towards a full policy re-plan. **b)** In a scenario where braking on its own might not be sufficient to avoid collision ( $v_0 = 25 \text{ ms}^{-1}$ , 1 s time gap), the model selects a policy that involves both braking and steering towards the opposite lane (see the model's selected policies in the topmost plots). **c)** The likelihood of the ego vehicle deciding to brake and stay behind the leading other vehicle (without any steering) as a function of time gap, with the four lines representing four different velocities (ranging from  $10 \text{ ms}^{-1}$  to  $25 \text{ ms}^{-1}$ ; the lines representing  $20 \text{ m/s}$  and  $25 \text{ m/s}$  are overlapping at zero brake only probability). This data include those samples where the agent is only steering. **d)** The relationship between the time gap and the brake response time of the ego agent in 280 model simulations (see Supplementary Materials 1.3.1). Regression line based on a meta-analysis of human brake response times [53] is shown for reference. **e)** The relationship of the inverse time-to-collision (TTC) at brake onset (defined as  $\frac{\max\{0, v_{\text{ego}} - v_{\text{oov}}\}}{\Delta x}$ ) and the lowest observed deceleration. Regression line based on the human deceleration magnitude data [14] is shown for reference. Video replays of the example simulations are available in the supplementary information.

same time (for instance, Figure 3b). Here, due to the smaller initial distance, the model’s perception delay was noticeably shorter (being only about 0.2 s, with the modeled agent perceiving the braking at  $t = 1$  s, the first dashed line). However, due to the more challenging initial kinematics, it was more difficult for the model to avoid collision, despite the shorter perception delay. In particular, the model switched between different policies four times. Initially, the model recognized the need to slightly brake and steer around the other vehicle: already at the time of the first re-plan ( $t = 1.4$  s, second dashed line) the collision component of EFE was substantially reduced by the chosen policy. This policy was mostly sufficient in improving the collision component of the pragmatic value, but as visible in the top panel (planned trajectory  $\tilde{\mathbf{X}}_{\text{ego}}$ ), the agent intends to stay in between lanes for an extended period. This led to two further re-plans ( $t = 3.2$  s and  $t = 3.8$  s, third and fourth dashed lines respectively) to adjust the trajectory. However, even having passed the other vehicle already, the model is not completely successful, with a noticeable lateral position component remaining in the pragmatic value. As the optimal solution of driving in the center of the current lane on a free road should have maximized the pragmatic value, this remaining lateral error is likely the result of the cross-entropy method not identifying the optimal policy. This represents a bounded planning capacity which, as discussed above, is also present in humans [13, 49–52] and thus an intended feature of our model.

By systematically varying the initial kinematics of the vehicles, we assessed the model behavior across a spectrum of front-to-rear scenarios. Due to the stochasticity of the model (foremost in behavior prediction and policy sampling), for each of the 28 sets of initial conditions we ran the simulation of the front-to-rear scenario 10 times. Based on these simulations, we analyzed the model’s chosen evasive maneuver, response time, and deceleration magnitude and compared it to human data reported in the driver behavior literature.

Figure 3c shows the probability that the model will brake only (without steering) for different velocities and time gaps. Existing studies on how human evasive maneuver choice depends on scenario kinematics in front-to-rear scenarios are limited. Thus, we compared our model results to

the few related studies that exist, but these do not provide sufficiently detailed analyses for rigorously evaluating our model’s evasive maneuvering decisions. These studies generally suggest that evasive maneuver decisions, similar to response timing, depend on the scenario kinematics (see [56] for a review). Avoiding collisions is generally kinematically more feasible by braking at lower speeds and by steering at higher speeds [57] and human drivers tend to swerve into an adjacent lane if a kinematically viable escape path exists [58–60]. In line with these general observations, our model prefers braking at lower velocities and favors combined swerving-and-braking or swerving only responses at higher velocities, regardless of the time gap (Figure 3c). At medium velocities ( $15 \text{ ms}^{-1}$ ) the model behavior is sensitive to the gap between the vehicles: the longer the time gap, the higher the probability of a brake-only maneuver. This pattern reflects a trade-off between the components of the pragmatic values associated with collisions, control effort (harshness of braking and steering), and lateral position. This dependence of swerving choice on time gap at intermediate speeds has, to our knowledge, not been empirically tested and represents an interesting quantitative prediction from our model. In more urgent scenarios (short time gaps), the model prefers swerving due to the low pragmatic value of harsh braking. Conversely, in less urgent scenarios (larger time gaps), the model opts for braking since moderate braking avoids collision without incurring the significant reduction of pragmatic value due to leaving the lane (while the deviation from the desired velocity is still tolerable at those medium speeds).

Regarding brake response times, empirical studies have consistently found a strong dependence on scenario kinematics [2, 3, 6, 14, 53, 61, 62]. Specifically, more kinematically urgent scenarios (e.g., with a small initial time gap and/or hard lead vehicle braking) lead to shorter response times while less urgent scenarios lead to longer response times, with approximately linear relationship between measures of urgency (e.g., the initial time gap) and mean response time [6, 53]. Our model produced behavior that is remarkably consistent with these findings (Figure 3d). Interestingly, compared to the evasive maneuver decisions, velocities do not seem to significantly influence brake response times, nor does the final

chosen behavior. Furthermore, model response times remain consistent (approx. 1 s) over the range of short time gaps (0.5 s to 1.5 s). This last result could be a consequence of the evidence accumulation mechanism requiring certain minimum time to trigger a re-plan even at a very high rate of incoming evidence. Relatedly, the lack of fast enough responses at short time gaps is a likely explanation for the collisions observed in the model (only at the shortest time gap of 0.5 s). However, because the data reported in the literature does not cover such short time gaps, this model prediction remains to be tested in future studies.

While response selection and its timing are comprehensively characterized by the choice of evasive maneuver and response times, response execution is a dynamic process and can be characterized by a variety of metrics. Here we focus on deceleration magnitude, which has been previously shown to depend on the kinematics of the front-to-rear scenario: human drivers brake harder in more kinematically urgent scenarios [14]. Our model captured this phenomenon: the magnitude of its braking increased with the inverse time-to-collision at brake onset (Figure 3e). This behavior of the model can be explained by the pragmatic value trade-off between avoiding a collision on the one hand and avoiding the effort of hard braking and losing velocity on the other hand. In other words, the model aimed to not brake harder than necessary to avoid collision.

### Opposite-direction lateral incursion scenario

For evaluating model behavior in the opposite-direction lateral incursion scenario, we used human data from a driving simulator study at the University of Leeds, UK, reported by Johnson et al. [56]. In this study, vehicles initially approached each other in opposite lanes when the computer controlled vehicle unexpectedly steered toward the participant's lane along a predefined path. The study implemented three kinematic variants differing in incursion "steepness": (1) a *steep* incursion crossing in front of the participant at a sharp angle and allowing a relatively easy escape by steering toward the opposite lane; (2) a *medium* incursion at a shallower angle, heading directly toward the participant; (3) a *shallow*

incursion only partially entering the participant's lane, making it possible to find an escape path by steering slightly toward the shoulder (the original study used left-hand traffic, so we are here avoiding directional terms to prevent confusion).

We re-implemented a reversed (i.e., right-hand traffic) versions of these scenarios in our simulator setup (see Supplementary Materials Figure A1), enabling a direct comparison between human and model behavior in an nearly identical scenarios. An example of our model implemented in the steep scenario is shown in (Figure 4a) and (Figure 4b) shows an example of the medium scenario (Figure 4b). When looking at the example simulations (Figure 4a and b), we can observe again that the model needs multiple re-plans before deciding on the final avoidance maneuver. Compared to the front-to-rear scenario, where this is likely caused by the model's bounded planning capacity, here this is due to the high uncertainty when predicting the positions of the other vehicles, which can be seen in the depictions on the top. In Figure 4a (steep incursion), a first re-planning is triggered at 4.2 s (first dashed line) but this does not significantly reduce the negative collision component of the pragmatic value. Additionally, the model neither initiates large steering maneuvers nor significant accelerations/decelerations. Together, this suggests that the high uncertainty about the other vehicle's behavior prevents the agent from finding an evasive policy that is better (has lower EFE) than the current policy, instead delaying the decision. The reason for this is that due to the wide spread in the belief about possible future trajectories that the oncoming vehicle may take, there is yet no evasive policy with lower EFE than the current non-evasive policy. With the collision risk unresolved after the first re-plan, surprise quickly accumulates toward a second re-plan at 4.6 s (second dashed line). By this time, the agents are closer, allowing less space for uncertainty to grow and enabling the model to identify a steering policy that mitigates the collision risk (after the second re-plan, the collision component of the pragmatic value no longer significantly contributes to surprise accumulation). The decision to swerve toward the left is a result of both the other vehicle having crossed sufficiently over to the right side to leave a gap for swerving, and the model's stronger preference for moving into the opposite

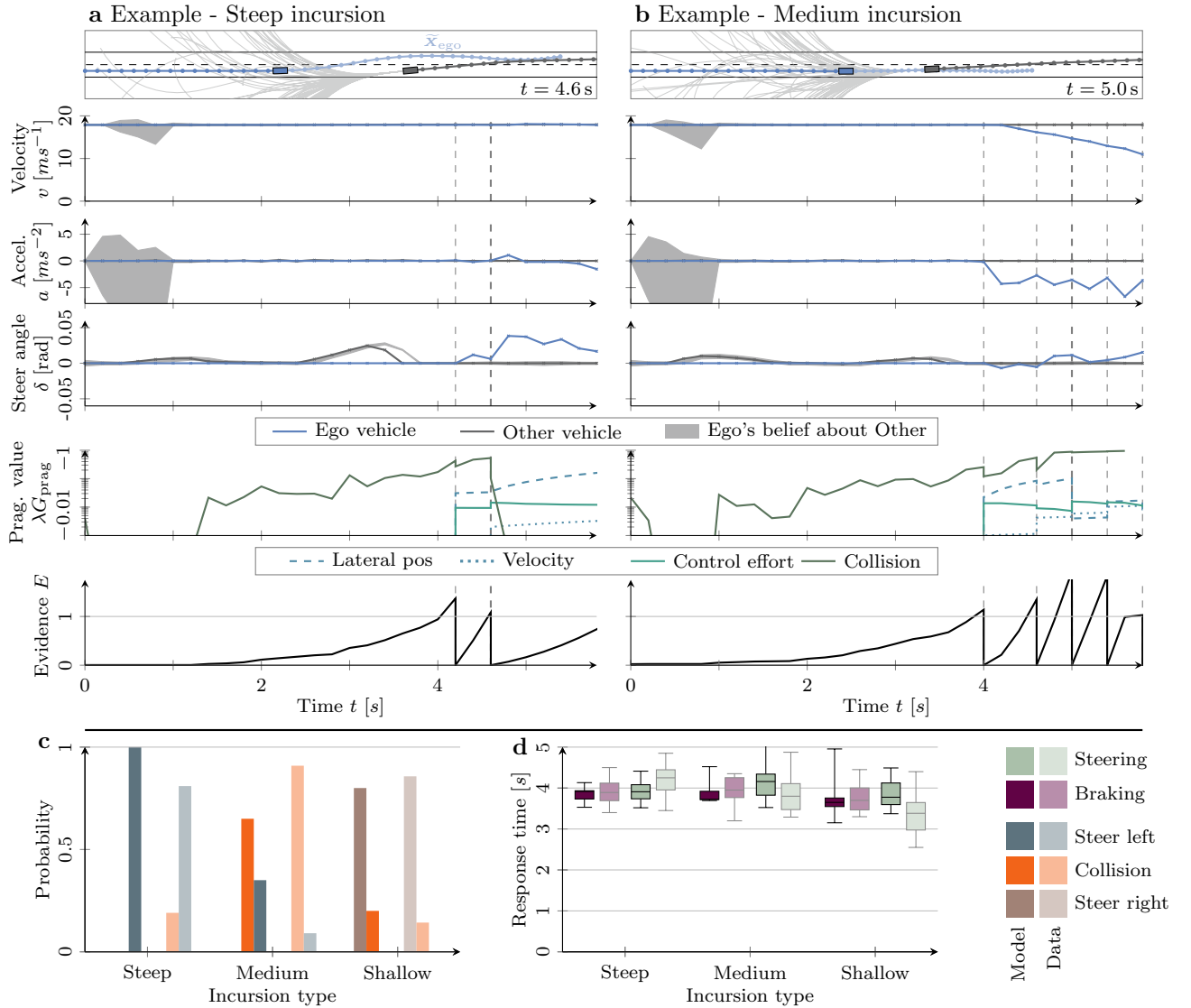


**Fig. 4:** Evaluation of the model in the opposite-direction lateral incursion scenario. **a)** A steep, unprompted incursion by the other vehicle leads to the model swerving towards the opposite lane. The sub-panels visualize the dynamics of both vehicles' velocity  $v$ , acceleration  $a$ , steering angle  $\delta$  and (for the ego vehicle) the components of the pragmatic value  $G_{\text{prag}}$  (scaled with the evidence accumulation gain  $\lambda$ ) that underlie the accumulated evidence towards a full policy re-plan. **b)** In response to a medium incursion by the other vehicle, where the model crashed at  $t = 5.8\text{ s}$ . **c)** The likelihood of the ego vehicle successfully avoiding the other vehicle by steering left (toward the opposite lane) or right (toward the shoulder), or failing to avoid a collision. **d)** Brake and steer response times. In panels C and D, human behavior and response times measured in a driving simulator study [56] are shown for reference. Video replays of the example simulations are available in the supplementary information.

lane over leaving the road to the right (similar to Figure 1). However, it can be seen in Figure 4a that this trajectory is not optimal. Namely, as can be seen in the top plot, the planned trajectory  $\mathbf{X}_{\text{ego}}$  chosen during the second re-plan at  $t = 4.6$  s (second dashed line) stays in the oncoming lane, resulting in a low value for the lateral position component of the pragmatic value. Consequently, slight course corrections will likely be performed later (but this would occur outside the current simulation window).

Figure 4b shows an example of the medium incursion scenario where the model is unable to avoid a collision. Again, likely due to uncertainty about the other vehicle’s behavior, the first re-plan at  $t = 4.0$  s (first dashed line) mainly results in a sharp deceleration and minor steering towards the right (i.e., towards the shoulder). While steering towards the right might seem suboptimal given the other agent’s current path, it aligns with the influence of the norm-conditioned particle filter, which – by weighing those particles returning to the other vehicle’s original lane higher in the EFE calculation – biases the model toward believing the other agent will return to its original lane (for more details on this, see the following section). At the second re-plan ( $t = 4.6$  s, second dashed line), the model abandons the steering to the right and steers slightly to the left but mainly just continues braking. However, this only marginally improves the collision components of the pragmatic value, leaving the imminent collision risk unresolved. By the third re-plan at 5 s (third dashed line), the agent continues braking, trying to minimize the impact severity, as by this point, the vehicles, which are as seen in the top panel still on a direct collision course with nearly no offset, got so close that a collision becomes nearly unavoidable. Consequently, even the fourth re-plan ( $t = 5.4$  s, fourth dashed line) fails to find a satisfactory trajectory, with the fifth re-plan coinciding with the collision at  $t = 5.8$  s (fifth dashed line).

As described above, we compared our model to the human data collected in the driving simulator study by Johnson et al. [56]. We closely replicated the scenarios of that study in our simulations (see Supplementary Materials 1.3.2), which allowed direct comparisons between the model and the data with respect to the chosen avoidance behavior and both braking and swerving

response times (which were extracted using the same method; see the Methods section). A key finding of Johnson et al. [56] was that the participants’ evasive maneuvering patterns and collision outcomes were strongly determined by the different scenario kinematics in the three incursion scenarios. In the steep scenario, most participants avoided collisions by steering toward the opposite lane, while in the shallow scenario, participants typically steered toward the shoulder, passing the other vehicle on the “inside”. However, in the medium scenario, the majority of participants collided with the oncoming vehicle. Since the urgency (i.e., time to collision at the initial steering of the oncoming vehicle) was constant across scenarios, the high crash rate in the medium case was attributed to greater uncertainty about the other vehicle’s future path, leaving no clear escape route.

As shown in Figure 4c, our model reproduced these results, reliably avoiding collisions in the steep and shallow scenarios through steering respectively left (toward the center) or right (toward the shoulder). Interestingly, the model also reproduced the human propensity for collision (although at slightly lower rate) in the medium scenario. Johnson et al. [56] suggested that, conceptually, a key reason why human drivers tended to collide in the medium incursion scenario is the high perceived uncertainty about the oncoming vehicle’s future behavior which prevents the driver from finding a sufficiently certain escape path. As described above, the current model offers a detailed computational account for the possible mechanisms underlying this phenomenon: the wide spread (uncertainty) in the behavior predictions about the oncoming vehicle, as well as a bias towards expecting that it will return to its own lane due to the norm-conditioning of the beliefs, prevents the model to find an evasive policy in time to avoid collision (see Figure 4b above). An additional factor behind the observed collision rates was likely also the model’s bounded planning capacity. Increasing the model’s planning capacity – by increasing the number of evaluated policies in the cross entropy method tenfold – resulted in a significant drop in the model’s collision rate (from 65% to 50% in the medium incursion scenario, and from 20% to 0% in the shallow incursion).

Furthermore, Johnson et al. [56] found that braking and steering response times – measured

from initiation of the incursion to the first reaction – were generally long, ranging around 3.5 to 4 seconds. While braking response times did not vary noticeably with incursion severity, steering response did decrease consistently from the *steep* towards the *shallow* scenario. Our model generally reproduced the range of response times, with closely matched median values (Figure 4d), but did not capture the variation in steering response times. One possible explanation may lie in the many participants avoiding collision in the steep scenario primarily by braking before making a final steering adjustment, delaying their recorded steering response. In contrast, the model relied more on steering for collision avoidance, requiring an earlier response. The underlying reason for these behavioral differences between the model and human drivers are still unclear but may have to do with varying individual preferences for braking versus swerving. Further work is needed to see if these individual differences can be reproduced by the model by varying its velocity-, lane change- and lateral control effort preferences.

## Evaluating individual model mechanisms

Comparison to the empirical data (Figures 3 and 4) revealed that our model captured the key aspects of human collision avoidance performance in the two collision avoidance scenarios. To better understand which of the model mechanisms are essential for capturing the empirical observations, we evaluated the performance of six simpler models which systematically excluded the key mechanisms one-by-one (Figure 5).

**Removing evidence accumulation.** Without evidence accumulation, the model fully replans its policy at every time step. Consequently, it starts reacting to changes in the other vehicle’s behavior immediately after detecting them. This resulted in a drastic reduction in response times across all scenarios (Figure 5b). Additionally, the model without evidence accumulation predominantly failed to avoid collisions in the shallow incursion scenario, contrasting sharply with human data and the full model. This was mostly caused by the model initiating braking very early. Given the uncertainty about the other vehicle, neither steering left nor steering right allows safe

escape paths, so the agent continues braking, coming to a complete stop. At the point in time where the certainty about the other agent is low enough for safely choosing either left or right, the agent can physically no longer avoid a collision (as it can not move laterally when stopped). An example simulation of this scenario can be found in the supplementary material. The fact that collisions happened mostly in the shallow incursion scenarios is likely because in the medium and steep incursion scenarios, early braking leaves enough space in front of the ego agent for the other vehicle to move across, which is not the case in the shallow incursion. In this scenario, collision would still occur if the ego agent stayed in its starting lateral position, which makes braking an insufficient avoidance mechanism. Based on those observations, the inclusion of evidence accumulation is critical for accounting for empirical data on human response times in both scenarios, as well as evasive maneuver selection in the shallow lateral incursion scenario.

**Removing added noise in behavior prediction.** The model that uses deterministic predictions about the other vehicle produced response times in the front-to-rear scenario that are only slightly longer than for both the full model and the human data (Figure 5c), especially given shorter time-gaps. By contrast, in the opposite direction lateral incursion scenario, it exhibited substantially shorter response times. The reason for this apparent discrepancy is that in the front-to-rear scenario, prediction noise results in ego agent’s believing that the other vehicle may brake more aggressively, prompting the model to react earlier. In the lateral incursion scenario, however, removing the prediction noise decreases ego agent’s uncertainty about the other vehicle, leading to earlier steering responses which, given how these particular scenarios unfolded, turned out to be a more effective avoidance strategy, as evidenced by the absence of collisions in this case. However, it should be noted that this strategy was only more effective after the fact (i.e., with hindsight of how the scenario played out). In another counterfactual scenario, where the oncoming vehicle turns back into its own lane, early swerving could instead result in collision (see [56] for further discussion of this important point).

Prediction noise affected not only response times but also the model’s choice of evasive

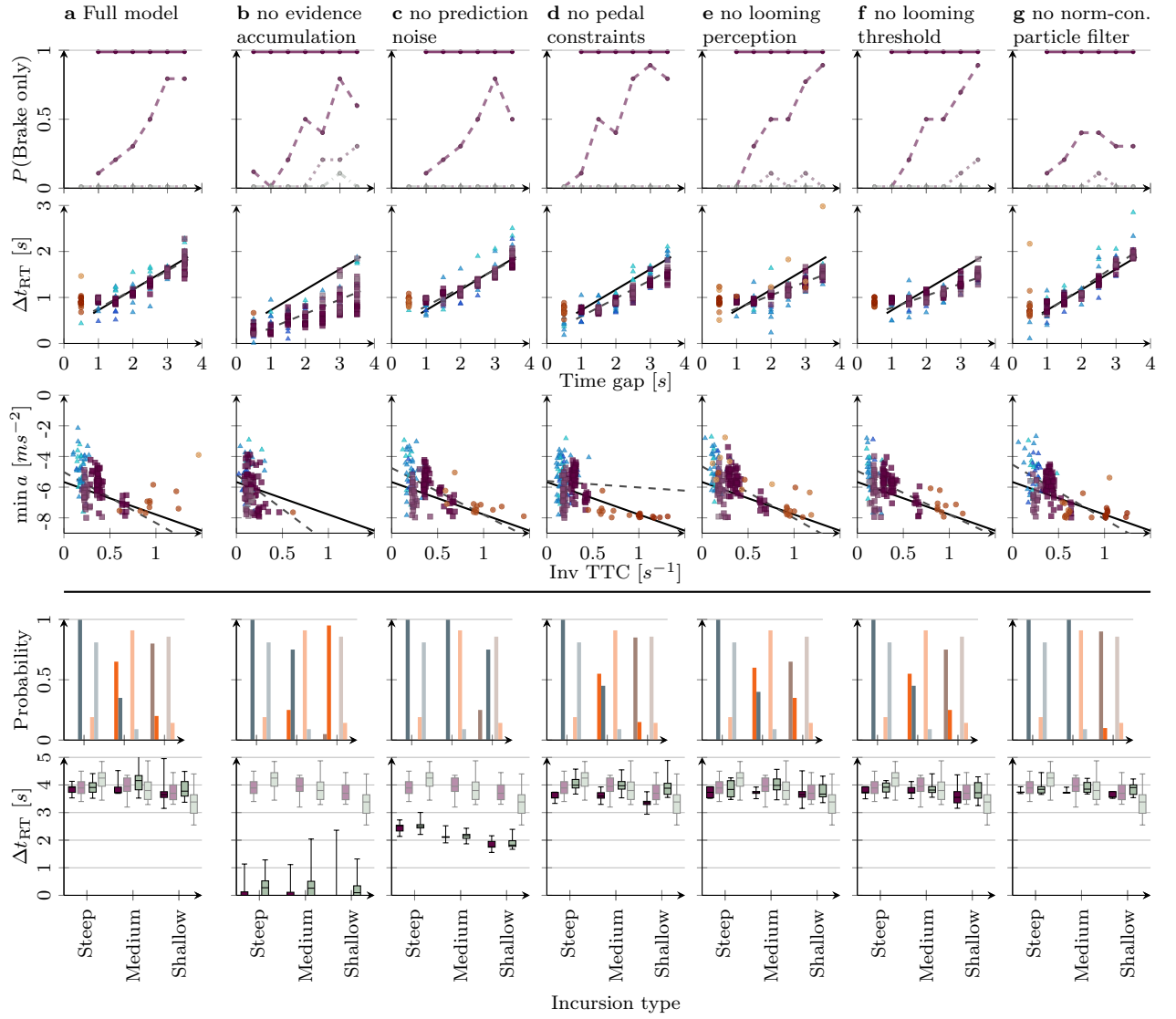


**Fig. 5:** Evaluation of variants of the model without some of its key mechanisms in the front-to-rear scenario (top three rows, see Figure 3 for the legend) and the lateral incursion scenario (bottom two rows, see Figure 4 for the legend). In the second and third rows, dashed gray lines depict regressions to model simulation results.

maneuver in the lateral incursion scenario. In particular, the model with deterministic predictions predominantly opted to avoid the other vehicle by steering left regardless of the incursion profile. This allowed the model to avoid collisions in all simulations, but is not consistent with the human data. Overall, these findings underscore that behavior prediction noise is crucial for accurately reproducing human behavior particularly in the lateral incursion scenario, and also confirms

the importance of enabling the model to account for uncertainty in its predictions to represent the key collision mechanism in the medium incursion scenario, as discussed in relation to Figure 4b.

**Removing pedal constraints.** The model not constrained by pedal switching delays resulted in approximately 0.2 s faster brake response times in both the front-to-rear and lateral incursion scenarios compared to the full model (Figure 5d). This matches the delay of 0.2 s implemented for

the switch from acceleration to deceleration. This delay could potentially be accounted for without pedal constraints by slightly decreasing the gain factor in the evidence accumulation mechanism. This approach would, however, also lead to increased steering response times in the lateral incursion scenario, which both in the full model and this ablation were already slightly slower than the human data. Thus, we deemed these constraints essential for describing human response times in the front-to-rear scenario.

**Removing looming perception.** We analyzed a version of the model which directly perceived kinematic variables without relying on looming (Figure 5e) as well as one which perceived looming but did not have a looming perception threshold (Figure 5f). In the front-to-rear scenario, both these models differed from the full model and the human data in that they produced faster brake response times at longer time gaps. For the model without the looming threshold, this is due to the fact that greater time gaps (and therefore greater distances) require a larger velocity difference to surpass the looming detection threshold, which delays responses, as it needs more time to accumulate. Furthermore, these results being very similar to the model that did not perceive looming at all (Figure 5e) indicates that in this scenario, the looming threshold was a key factor behind the ability of the model to capture human response times. Additionally, while not specifically analyzed here, this effect is expected to be exacerbated in high speed freeway scenarios where (given the higher speed) the following distances for a given time gap increase, further emphasizing the importance that the model accounts for this phenomenon. In the opposite direction lateral incursion scenario, removing the looming threshold (or looming entirely) did not have any major effect, as the high relative velocities overcome the looming threshold very early, and perception accuracy of longitudinal positions is far less relevant in that scenario.

In summary, models without either looming perception or looming threshold resulted in qualitative differences between the model and human data on brake response times in the front-to-rear scenario and collision rates in the lateral incursion scenario. This highlights the importance of both looming-based perception and looming perception

threshold, in addition to the strong theoretical support.

**Removing the norm-conditioned particle filter.** In the model without the norm-conditioned particle filter, the changes to the overall behavior in the front-to-rear scenario are very minor compared to the full model (Figure 5g). However, in the lateral incursion scenario this change has a major impact on the collision outcome in the medium incursion scenario, where the model now avoids collision in all runs, similar to the model variant without prediction noise. When the norm-conditioning is removed, the model treats all predicted trajectories as equally likely instead of initially focusing on those where the oncoming vehicle returns to its own lane. This assumption, together with the reduced pragmatic value associated with lane changes, leads the full model to initially steer towards the right, costing valuable time and creating situations where steering to the left is no longer a viable solution, and collisions become unavoidable. By contrast, in the model without norm conditioning, potential collisions along steeper incursion trajectories are taken more seriously earlier, making an initial steering to the right less likely. Instead, the model without norm conditioning more frequently evades to the left immediately in such medium incursion scenarios, resulting in the observed lack of collisions. This aligns with the hypothesized role of norm conditioning in crashes, as discussed in connection with Figure 4b.

While these differences already highlight the importance of the norm-conditioned particle filter, it has the strongest impact in benign (non-conflict) scenarios. In such scenarios, the model with the simple kinematics-based behavior prediction mechanism is unrealistically conservative due to having to plan for all kinematically possible futures of the other vehicle — a problem that is avoided by the model with norm-conditioned particle filter (see Supplementary Materials 1.4 for an example).

Overall, all six simpler versions of the model exhibit qualitative differences compared to the full model, and none capture the human data across both scenarios as comprehensively as the full model. This provides evidence that all of the analyzed model mechanisms are all important for capturing human collision avoidance behavior.

Additionally, we ran a model ablation where we ignored the epistemic value when selecting policies, which however did not result in any meaningful differences.

## Discussion

Building on previous work [33], we here presented an active inference-based framework for modeling human collision avoidance behavior based on first principles. To our knowledge, this is the first published computational model that offers a detailed account of human collision avoidance behavior across multiple conflict scenarios. Our model reproduces many key results in the rich literature on collision avoidance in front-to-rear scenarios, in particular the dependence of response times and braking magnitude on scenario kinematics. The model also generated several detailed predictions on how evasive maneuver decisions (braking vs. swerving) vary with scenario kinematics which can be tested in future experiments. Furthermore, we compared the model directly to human behavior in an opposite-direction lateral incursion scenario with varying kinematics obtained in a driving simulator study [56]. This analysis demonstrated that the model can reproduce human evasive maneuver decisions, collision outcomes, as well as response times in the different incursion scenarios.

A key novel feature of our model is its ability to flexibly represent closed-loop collision avoidance through dynamic replanning of policies, including braking, steering, and accelerating actions, in a way that is qualitatively and quantitatively similar to human collision avoidance behavior. In contrast, existing publicly available collision avoidance models either implement a "one-shot", often predetermined, open-loop evasive maneuver [1, 5, 63] or limited aspects of closed-loop control, such as intermittent braking but no steering [11, 64]. Some commercially available models – the Stochastic Cognitive Model (BMW; [65, 66]), the driveBOT model (cogniBIT; [67, 68]) – reportedly implement human-like closed-loop behavior in collision avoidance scenarios. However, the lack of available information on the detailed working principles of these models precludes a meaningful comparison with the current model.

Our model achieves closed-loop behavior by continuously evaluating evasive policies based on

their expected free energy, pursuing the policy with the lowest EFE, and allowing for further replanning if the chosen policy turns out to not yield the preferred (and hence expected) outcomes (e.g., due to limited planning accuracy or unexpected changes in how the scenario unfolds). This, in effect, implements a constraint satisfaction mechanism where different model preferences are traded against each other in finding the policy with the highest overall combined pragmatic value and epistemic value. We observed several examples of this (Figures 3 and 5) where, for example, the model generally prefers to brake at low speeds (since the loss related to the preferred speed is not as high as the cost of changing lane) and swerve at higher speeds (where the cost of braking in terms of speed loss are higher). This yields detailed predictions of human behaviors in different kinematic situations that could be further tested empirically.

Another important novel aspect of our model is its ability to dynamically account for uncertainty about the future behavior of other agents. This is particularly important in situations like the lateral incursion scenario where the driver cannot determine *a priori* if the other vehicle will continue crossing the ego vehicle's lane or if it will turn back to its original lane, resulting in a wide range of potential future trajectories of the other vehicle. However, the uncertainty may be reduced as the scenario unfolds, opening up new available escape paths, or *escape affordances* [56], as was the case in the current steep and shallow incursion scenarios. In such cases, a too early evasive response may be premature (and non-optimal) and does not properly reflect human behavior. We saw an example of this in Figure 5c, where the model without prediction noise responded much faster than humans and the full model, thus avoiding collision in all cases. However, such overconfident evasive maneuvering behavior would be detrimental in the alternative scenario where the other vehicle is turning back into its original lane. By representing the uncertainty about the other vehicle's future positions using a vehicle dynamics (bicycle) model and a noisy particle filter, our model is able to handle such situations and successfully reproduce human behavior.

It should be noted that in the collision avoidance scenarios simulated in the present study, there is little opportunity for the driver to reduce the uncertainty about the oncoming vehicle's

future trajectory through epistemic actions. In other words, there is little the driver can do to obtain further information that could help predict what the other vehicle will do. However, as further discussed below, in the real world communicative acts such as honking, flashing headlights or initially moving to the right in the lane could serve to reduce uncertainty about the oncoming vehicle driver's intent, but since the oncoming agent was here assumed to be non-reactive such aspects were not addressed in the current work (this is a topic for future development of the model). Thus, as expected, disabling the epistemic value component of EFE did not significantly change the current simulation results.

While active inference models can be implemented computationally in many different ways, following [33], we used a stochastic receding-horizon control architecture as the basis for the implementation. This shares similarities with prior work in robotics, particularly decision-theoretic approaches that explicitly account for uncertainty in actuation and sensing by propagating belief states into the future, often using particle-based representations, and then selecting actions that optimize expected outcomes based on this projected belief evolution [69–71]. However, our work diverges from these engineering models in two crucial aspects. First, since our goal is to represent human driver behavior rather than designing a robotics controller, the modeling focuses on capturing key aspects of human driving, such as response timing and evasive maneuver decision making, rather than optimizing performance. Second, our modeled agent minimizes EFE (as prescribed by the active inference framework), while traditional state-based reward functions often employed in the control literature lack such a neuro-biologically plausible objective.

Our model incorporates an explicit mechanism for evidence accumulation to account for human response timing, based on existing models [6, 72? –74]. Evidence accumulation models naturally account for the situation-dependency of response timing in traffic situations: the faster a traffic conflict escalates, the faster the human's response to it [6, 14]. Compared to existing evidence accumulation models, our model introduces some key novel aspects. In particular, by contrast to traditional models that accumulate perceptual

evidence (e.g., looming [? ]), our model rather accumulates *surprise*. Similar ideas have been explored in existing models [6, 47, 64], based on the notion that a traffic conflict by definition is an extremely rare (and hence surprising) event which always takes place against a "default" expectation of how the situation would normally play out (Figure 1). This is also the key idea behind the NIEON (Non-Impaired driver with their Eyes ON the conflict) response time model which conceptualizes the onset of the stimulus that human drivers respond to in a traffic conflict as the onset of surprise (i.e., the violation of the initial default expectation) [6]. The current model generalizes this idea in several novel ways. First, instead of triggering a predefined action such as braking when the surprising evidence has reached the threshold, the evidence accumulation here triggers the *re-planning* of a new policy, using the EFE-based policy selection mechanism discussed above. Second, the surprise signal that is being accumulated is not just the difference between a predicted and actual signal but rather the negative pragmatic value of the current policy, that is, how "bad" the currently selected default policy is relative to the agent's preferred observations. This provides a straightforward solution to the known problem of how to determine whether a given surprise signal is *relevant* to the agent [47].

While we here model evidence accumulation explicitly, it can in principle be seen as an implicit feature of active inference [75]. However, in practice, it is challenging to accurately represent human response dynamics implicitly in a simplified model like ours and, in order to enable a straightforward tuning of the model's response performance to human data, we chose the current explicit modeling of evidence accumulation. As demonstrated by our simulation results (Figure 5b), the inclusion of this mechanism is essential to account for realistic response times in our model.

The current model is based on the general model predictive control architecture originally developed for the model of routine driving described in [33] which, in turn, is based on the standard discrete-time active inference EFE model for planning agents formulated as a partially observable Markov decision process [24]. The original routine driving model in [33] focused primarily on the role of epistemic value in resolving

uncertainty when driving around visual occlusions and during visual time sharing (drawing from the rat-in-a-T-maze example in [24]). However, that model was not aimed at describing time-critical behaviors. For instance, in collision avoidance scenarios its responses to sudden stimuli would be overly fast, similar to the version of our model without evidence accumulation (Figure 5b). Extending the original model [33] with not only evidence accumulation, but also other mechanisms such as looming-based perception and norm-conditioned predictions was essential for capturing human collision avoidance behavior (Figure 5). Otherwise, the model we reported here retains the key features of the original routine driving model needed for dealing with uncertainty resolution through epistemic action, thus offering a powerful and general computational framework for modeling driving behavior, also beyond collision avoidance. As in [33], we employed engineering tools like the cross-entropy method and particle filters with discrete and continuous variables. However, while relying on such established methods, our model does not reduce to a combination of them; instead, these methods serve as means for implementing specific cognitive mechanisms within our active inference framework.

Our framework is grounded not only in active inference and the free energy principle [26], but also enactivist approaches to cognitive science [76, 77]. Active inference and enactivist cognitive science share the the foundational notion that behavior in biological agents results from a self-organizing process geared towards sustaining the agent’s integrity (existence) over time. This emphasizes a strong continuity between life and mind [77–79] and offers a natural solution to the problem how the certain aspects of the environment become *meaningful* and *relevant* to an agent [80]. Such an *existential imperative* can be described as the organism striving to maintain itself in a sparse attractive set of preferred agent-environment states, where the attractive set depends on the specific organism in question. Thus, to survive over time, a fish needs to remain in water with the right chemical balance and temperature range, obtain food, avoid being eaten by certain predators etc. This implies that these particular states are meaningful and relevant to the fish which then acts in order to observe these

states with a high degree of certainty, thus looking as if it is minimizing free energy over time. By the same token, we endowed our model with a (highly simplified) set of preferred states that are meaningful and relevant to a human car driver (avoid danger of collision, stay on the road, keep up progress, avoid too harsh braking/steering) and defined the model such that it acts (selects and executes policies) in a way that maximizes the chance of observing these preferred states.

Related to this, our model also offers a novel operationalization of the classical notion of *affordance*, traditionally broadly defined by Gibson [35] as what the environment ”*offers the animal, what it provides or furnishes, either for good or ill*” (p. 127). Thus, when our model identifies candidate evasive policies associated with low EFE, these can be understood as affordances in the sense of opportunities for actions that are worth pursuing. The active inference framework offers a further distinction between *pragmatic affordances* yielding unsurprising, familiar and preferred observations and *epistemic affordances* yielding information that can resolve uncertainty about pragmatic affordances [33, 81, 82] (see [56]) for a further discussion about this expanded notion of affordances and its relation to the classical affordance concept in ecological psychology.

Thanks to its generality, active inference-based models have been developed for virtually every facet of biologically-based cognition and behavior, in organisms ranging from single cells [78], plants [83], individual animals and humans [84] to social and cultural phenomena [85], which provides a great source of concepts and ideas for modeling different aspects of human road user behavior. Thus, importantly, we see active inference not just as a computational approach to model development, but as a general theoretical framework for understanding road user behavior that can guide modeling at a conceptual level and generate novel hypotheses for experimental studies. At the same time, the great majority of existing active inference models use relatively simple toy scenarios, thereby limiting its applicability to real-world human behavior [9]. By operationalizing active inference in the context of a dynamically rich task, that is, collision avoidance and evaluating it against human data from both simulated and real-world driving, this study

pushes the boundaries of active inference applications toward the modeling of complex human naturalistic behaviors.

While, as discussed above, our model represents a significant advancement in human collision avoidance modeling, it has several limitations that can be addressed in future work. First, in this work we essentially hand-tuned the model parameters to fit the human data from the two collision avoidance scenarios. Whereas this highlights the model’s generalizability and interpretability, hand-tuning model parameters is impractical at scale. Future research should explore systematic parameter optimization methods, for example using the approach suggested by Wei *et al.* [86].

Second, the current model assumes that other agents are non-reactive, an assumption that in general case does not hold. Thus, future work incorporating reactive agents and investigating the role of communication in agent interactions driven by epistemic value could extend the model’s applicability, enabling simulations of interactions between multiple active inference agents. Moreover, the current model (as well as the original model in [33]) only reasons at a shallow “unsophisticated” level about how actions bring about future observations with varying degrees of uncertainty. Further work could explore the possibilities of incorporating *sophisticated inference* [87], which enables “deeper” levels of recursive reasoning about how future observations would lead to updated beliefs and corresponding new actions. This may be particularly relevant when modeling interactions between road users.

Third, the model currently only accounts for perceptual limitations in terms of visual looming, which, strictly speaking, only applies to objects located along a straight path of travel relative to the gaze direction of the observer (in our case, this means objects located straight ahead of the ego vehicle). Thus, to represent other types of perceptual limitations, alternative perceptual variables would need to be explored such as, for example bearing angle as a specification of perpendicular collision course [88].

Fourth, while mechanisms for dealing with partial observability during occlusions and visual time sharing were explored in [33], further work is needed to develop more comprehensive solutions for representing and reasoning about multiple

agents hidden behind occluding objects or appearing outside the driver’s field of view (see also Wei *et al.* [89]).

Finally, while the current policy sampling and kinematic-based particle filter approach was demonstrated to work well in the current scenarios, this could be a limiting factor in scaling the model to a wider range of scenarios, especially when modeling pre-conflict scenarios with more complex road infrastructures and road user interactions. To overcome this potential limitation, machine-learning-based generative models from existing data-driven models [17, 21, 90–94] could be leveraged to generate possible futures in the current model that are evaluated by EFE, either stand-alone or in combination with the current kinematic rollouts, thus potentially enhancing the generalizability of the model.

Overall, our work contributes to the recent body of research [33, 86] with new evidence that active inference can serve as a general framework for computational road user modeling. Along with the emerging real-world applications of active inference in robotics [95] and artificial intelligence [96], this work can aid the development of simulated agents used for real-world applications in advanced driver assistance systems and autonomous vehicle evaluation.

## Methods

### Model principles

Our model follows the architecture of the original model initially formulated by Engström *et al.* [33], and combines some of the original elements of that model with multiple new mechanisms. In particular, our model retains the representation of probabilistic beliefs using sets of samples and the correspondingly sample-based estimation of the expected free energy (see equation (6)) as well as the cross entropy method used for policy selection. In addition to these mechanisms, we introduced looming perception, evidence accumulation, the norm-conditioned particle filter, and the constraints on acceleration profiles (see Figure 5 for the analysis of the impact of these new mechanisms on model behavior). We also modified the Bayesian belief update (equation (2)) and the calculation of the epistemic value (equation (7)).

In our active inference model, the environment is represented by the *generative process*, with a state of the world  $\boldsymbol{\eta} \in \mathcal{E}$  which is partially observable by the agent. The agent can influence the environment with its actions  $\mathbf{a} \in \mathcal{A}$  (according to the state transition probability  $\hat{p}(\boldsymbol{\eta}'|\boldsymbol{\eta}, \mathbf{a})$ ), resulting in observations  $\mathbf{o} \in \mathcal{O}$ , whose dependence on the world state is described in  $\hat{p}(\mathbf{o}|\boldsymbol{\eta})$  (the  $\hat{p}$  is used to show these function be part of the *generative process*).

The agent has an internal model of the world, the *generative model*, with the corresponding partially observable state  $\mathbf{s} \in \mathcal{S}$ , and the corresponding state transition function  $p(\mathbf{s}'|\mathbf{s}, \mathbf{a})$  and observation probability  $p(\mathbf{o}|\mathbf{s})$ . As the *generative model* is an abstraction of the real world described by the *generative process*,  $\boldsymbol{\eta}$  and  $\mathbf{s}$  do not necessarily have to represent the same state spaces ( $\mathcal{E} \neq \mathcal{S}$ ). The agent is uncertain about the state of the generative model, represented by the probability density function  $q(\mathbf{s})$  (referred to as the agent's belief about the state  $\mathbf{s}$ ). Following [33], in our model the agent represents its belief distributions  $q(\mathbf{s})$  in a non-parametric way as a set of  $N$  samples  $\mathbf{S} = \{\mathbf{s}_1, \dots, \mathbf{s}_N\}$  (i.e., a particle filter).

The agent then tries to minimize its *free energy*, both in the belief  $q(\mathbf{s})$  it forms (*variational free energy*) and the actions  $\mathbf{a}$  it chooses (*expected free energy*). The action and policy selection is based on the existence of a preference prior  $p(\mathbf{o})$  depicting preferred observations.

## Perception

At time  $t$ , the agent perceives the world state  $\boldsymbol{\eta}_t$ , resulting in the observation  $\mathbf{o}_t$ :

$$\mathbf{o}_t \sim \hat{p}(\mathbf{o}'|\boldsymbol{\eta}_t) \quad (1)$$

With this observation, the agent updates its old belief  $q(\mathbf{s}_{t-1})$  to  $q(\mathbf{s}_t)$ . The active inference framework postulates that this update is based on the minimization of the *variational free energy* [24], but in our case we use standard Bayesian updating:

$$q(\mathbf{s}_t) \propto p(\mathbf{o}_t|\mathbf{s}_t) \mathbb{E}_{q(\mathbf{s}_{t-1})} p(\mathbf{s}_t|\mathbf{s}_{t-1}, \mathbf{a}_{t-1}). \quad (2)$$

Here, the particle filter first advances the individual samples in  $\mathbf{S}_{t-1}$  (representing  $q(\mathbf{s}_{t-1})$ ) using the transition function to

get the expected states  $\mathbf{S}_{A,t}$  (approximating  $q_A(\mathbf{s}_t) = \exp(\mathbb{E}_{q(\mathbf{s}_{t-1})} \ln p(\mathbf{s}_t|\mathbf{s}_{t-1}, \mathbf{a}_{t-1}))$ ), with  $\mathbf{s}_{A,t,n} \sim p(\mathbf{s}'|\mathbf{s}_{t-1,n}, \mathbf{a}_{t-1})$  being randomly sampled. Then, a kernel density estimate [97, 98] based on  $\mathbf{S}_{A,t}$  is used to approximate  $q_A(\mathbf{s}_t)$  as a Gaussian Mixture Model (GMM). Assuming that  $p(\mathbf{o}_t|\mathbf{s}_t)$  is Gaussian as well,  $q(\mathbf{s}_t)$  can also be represented as a GMM; this allows straightforward sampling of  $\mathbf{S}_t$ . Compared to the approach in the original model [33] of weighting samples  $\mathbf{s}_{A,t,n} \in \mathbf{S}_{A,t}$  with  $p(\mathbf{o}_t|\mathbf{s}_{A,t,n})$  and then resampling based thereon, this approach allowed us to represent large shifts in beliefs outside the extreme values of the initial set  $\mathbf{S}_0$ .

The agent's visual perception in our model is based on looming (Supplementary Materials 1.2.2) – the optical information immediately available to humans about the relative motion of objects straight ahead in the direction of travel [35]. Specifically, the relative position and motion of objects along the forward path of the agent is perceived in terms of the visual angle  $\varphi$  subtended by the object at the retina of the observer, and its derivative, the angular rate  $\dot{\varphi}$  (looming) [34, 40]. Due to the nonlinear relationship between the observer's distance to the observed vehicle (in Figure 2a referred to as  $\Delta x$ ) and  $\varphi$  (with increasing distances, equal variations  $\delta \Delta x$  lead to increasingly smaller  $\delta \varphi$ ), perception errors for  $\varphi$  and  $\dot{\varphi}$  will lead, respectively, to increasing inference errors and therefore uncertainty about the position and speed of the leading other vehicle at increasing distances. We represent this aspect in the model by setting the noise in  $p(\mathbf{o}|\mathbf{s})$  to be constant across  $\varphi$  and its derivatives.

At a certain distance,  $\dot{\varphi}$  is no longer perceptible to the human eye, which implies a minimal threshold for looming detection [41, 42]. To account for this, the model incorporates a detection threshold on  $\dot{\varphi}$  (i.e., for small  $|\dot{\varphi}|$ , the means of the observation probabilities  $p(\mathbf{o}|\mathbf{s})$  for velocities and acceleration were set to the values corresponding to  $\dot{\varphi} = 0$ ). This means that changes in the other vehicle's velocity cannot be perceived by a human driver beyond a certain distance, resulting for example in a delayed recognition if the lead vehicle suddenly brakes.

## Behavior prediction

After observing the current state of the world, the agent applies the state transition function  $p(\mathbf{s}'|\mathbf{s}, \mathbf{a})$  starting from its current belief  $q(\mathbf{s}_t)$  in order to generate a predicted belief about the future states of the situation  $\tilde{q}_s(\mathbf{s}_\tau|\boldsymbol{\pi}_t, q(\mathbf{s}_t))$  (with  $\tau \in \{t+1, \dots, t+H\}$ , an arbitrary policy  $\boldsymbol{\pi}$  containing the ego agents sequence of planned actions, and prediction horizon  $H$ ) of agents in the scene, as well as the corresponding belief over possible future observations  $\tilde{q}_o(\mathbf{o}_\tau|\boldsymbol{\pi}_t, q(\mathbf{s}_t)) = \mathbb{E}_{\tilde{q}_s(\mathbf{s}_\tau|\boldsymbol{\pi}_t, q(\mathbf{s}_t))} p(\mathbf{o}_\tau|\mathbf{s}_\tau)$ . During this prediction process, the agent adds noise to the control inputs of the other agents to represent the possibility that they might change their behavior.

Practically, the agent advances the belief  $\tilde{q}_s(\mathbf{s}_\tau|\boldsymbol{\pi}_t, q(\mathbf{s}_t))$  (represented by  $\tilde{\mathbf{S}}_\tau = \{\mathbf{s}_{\tau,1}, \dots, \mathbf{s}_{\tau,N}\}$ ) to the next time-step by using the state transition function (in our case based on a bicycle model [99], see Supplementary Materials 1.2.1) on each of the sample states  $\mathbf{s}_{\tau,n} \sim p(\mathbf{s}_\tau|\mathbf{s}_{\tau-1,n}, \mathbf{a}_{\tau-1})$ , and applies additive noise (similarly to forming the expected belief  $q_A(\mathbf{s})$  in the belief update). The belief  $\tilde{q}_o(\mathbf{o}_\tau|\boldsymbol{\pi}_t, q(\mathbf{s}_t))$  is then represented by the set  $\tilde{\mathbf{O}}_\tau = \{\mathbf{o}_{\tau,1}, \dots, \mathbf{o}_{\tau,N}\}$ , where  $\mathbf{o}_{\tau,n} \sim p(\mathbf{o}_\tau|\mathbf{s}_{\tau,n})$ .

It could be noted that this belief propagation scheme is *unsophisticated* in the technical sense that it does not condition the beliefs about future states on corresponding counterfactual observations. While it would theoretically be possible to use a form of *sophisticated* inference [87] that accounts for such conditioning, we here used the unsophisticated approach for simplicity, similar to the original model [33] and most existing active inference models.

A key advantage of this kinematics-based behavior prediction approach (compared to machine learning-based data-driven approaches) is that in a collision avoidance scenario it allows the model to account for kinematically possible but low-probability “extreme” (long-tail) behaviors of other agent once the conflict has been initiated, something which is hard to learn based on data. However, on the flip side, this could yield too pessimistic behavior predictions prior to the conflict. For example, if the noise in the particle filter is high, leading to a high dispersion of the particles, the model operates based on

the belief that, for example, any oncoming vehicle may encroach into their lane at any time. This leads to overly reactive behaviors. Human drivers, by contrast, typically avoid such pessimistic predictions by assuming that other drivers will adhere to road rules and other established traffic norms [44, 45]; for example, they typically assume that oncoming vehicles will stay in their lane unless there is evidence to the contrary. Without such an assumption driving on roads with multiple adjacent lanes would not be possible.

To address this issue, we introduced the normative probability density function,  $p_n : \mathcal{O} \rightarrow (0, 1]$ , reflecting expectations about adherence to traffic norms, by assigning lower probability values to future observations that violate established norms (such as leaving the lane). Thereby, we implement an assumption into the model that other road users will behave according to such norms. While beliefs about traffic norms could also be implemented directly in the state transition function  $p(\mathbf{s}'|\mathbf{s}, \mathbf{a})$ , we here chose this simpler approach which was deemed sufficient for present purposes. This possibility can be explored in future work.

Specifically, we normalize the probability densities  $p_n(\mathbf{o}_\tau)$  across the  $N$  particles in  $\tilde{\mathbf{O}}_\tau$  that represent  $\tilde{q}_o(\mathbf{o}_\tau|\boldsymbol{\pi}_t, q(\mathbf{s}_t))$ . This ensures that when normative behavior is no longer observed (i.e., all values of  $p_n(\mathbf{o}_\tau)$  for  $\mathbf{o}_\tau \in \tilde{\mathbf{O}}_\tau$  are similarly low), norm violations are still treated as likely events requiring an appropriate response. Specifically, as there are no norm-compliant particles to dominate onto the EFE calculation, the norm-violating particles will now all be considered with similar importance. This approach – which we call *norm-conditioned particle filter* – helps aligning the model’s predictions with realistic driving scenarios while allowing for the anticipation of norm violations when necessary. As traffic norms are typically scenario-specific, we defined them individually per scenario (Supplementary Materials 1.3.1 and 1.3.2).

## Policy sampling

Based on the predicted behavior of the other vehicle, the agent selects its policy  $\boldsymbol{\pi}$ . Here, policies are defined as sequences of  $H$  future actions; following the bicycle model, the actions are defined in terms of acceleration  $a_{\text{long}}$  and steering rate  $\omega$ .

These actions are selected using the cross-entropy method [33, 48], which iteratively resamples sets of  $M$  candidate policies  $K$  times, where the resampling focuses around the subset of the  $\beta M$  best samples from the previous iteration. Specifically, the agent takes the mean and variance of this promising subset (ignoring potential correlations), and then samples a new set with size  $M$  from the corresponding normal distribution. In contrast to the original model [33] that randomly picked the final sampling output from the last iteration’s set, here we specifically choose the best sample.

To better represent human behavior, the model incorporates a pedal constraint to filter out unrealistic changes in acceleration (Supplementary Materials 1.2.3). As human drivers generally control acceleration by operating the brake and gas pedal with a single foot and cannot move the foot between pedals instantaneously, the model imposes a constant holding time interval of 0.2 s at  $a_0 \lesssim 0 \text{ ms}^{-2}$ , such that if the model transitions from a current acceleration  $a_{\text{long}} > a_0$  to a target acceleration  $a_{\text{long},f} < a_0$ , it must first decelerate to  $a_0$ , maintain that value for 0.2 s, and then proceed to  $a_{\text{long},f}$ . The same applies for acceleration changes in the other direction.

## Policy roll-out and evaluation

To evaluate a policy  $\pi$ , the agent first uses the bicycle model to roll out its possible future states based on  $\pi$ . In the general case, the possible future states of the agent and the other vehicle are coupled, hence the agent rolls out its policies jointly with the predicted futures of the other vehicle. For the reason of simplicity, however, our model assumes that in  $p(\mathbf{s}'|\mathbf{s}, \mathbf{a})$  the other vehicle is unresponsive to the actions of the ego vehicle, allowing us to separate behavior prediction and policy roll-out.

Active inference then rests on the fundamental assumption that an agent prefers policies which minimize its *expected free energy* (EFE)  $G$  over the prediction horizon of  $H$  time steps (i.e., the best policy is the one with the lowest EFE). This EFE combines the desire of the agent to, on the one hand, observe itself in states that it prefers (maximize pragmatic value  $g_{\text{pragm}}$ ) and, on the other hand, seek information that may reduce uncertainty about the world (maximize epistemic value

$g_{\text{epist}}$ ):

$$G(\boldsymbol{\pi}_t, q(\mathbf{s}_t)) = \sum_{\tau=t+1}^{t+H} -g_{\text{pragm}}(\tilde{q}_o(\mathbf{o}_\tau | \boldsymbol{\pi}_t, q(\mathbf{s}_t))) - g_{\text{epist}}(\tilde{q}_s(\mathbf{s}_\tau | \boldsymbol{\pi}_t, q(\mathbf{s}_t))). \quad (3)$$

The pragmatic values  $g_{\text{pragm}}$  is defined as

$$g_{\text{pragm}}(\tilde{q}_o(\mathbf{o})) = \mathbb{E}_{\tilde{q}_o(\mathbf{o})p_n(\mathbf{o})} \ln p(\mathbf{o}), \quad (4)$$

while we use the Shannon entropy  $\mathcal{H}$  to calculate the epistemic value [24]

$$\begin{aligned} g_{\text{epist}}(\tilde{q}_s(\mathbf{s})) &= \mathbb{E}_{\tilde{q}_s(\mathbf{s})} D_{KL}[\tilde{q}(\mathbf{s}|\mathbf{o})|\tilde{q}_s(\mathbf{s})] \\ &= \mathcal{H}(\mathbb{E}_{\tilde{q}_s(\mathbf{s})} p(\mathbf{o}|\mathbf{s})) - \mathbb{E}_{\tilde{q}_s(\mathbf{s})} \mathcal{H}(p(\mathbf{o}|\mathbf{s})). \end{aligned} \quad (5)$$

The first term in Equation (5) is known as the *posterior predictive entropy* and represents the extent to which a policy is expected to yield a variety of different observations. The second term, known as *expected ambiguity* represents the diversity of observations expected for a given state, that is, the extent to which the observations of that state are unreliable (e.g., due to reduced visibility).

In our particle-based representation, we represent  $\tilde{q}_s(\mathbf{s})$  with the set  $\tilde{\mathcal{S}}$  of  $N$  particles and  $\tilde{q}_o(\mathbf{o}) = \mathbb{E}_{\tilde{q}_s(\mathbf{s})} p(\mathbf{o}|\mathbf{s})$  with the set  $\tilde{\mathcal{O}}$ , resulting in the approximations

$$\tilde{g}_{\text{pragm}}(\tilde{\mathcal{O}}) = \frac{\sum_{\mathbf{o} \in \tilde{\mathcal{O}}} p_n(\mathbf{o}) \ln p(\mathbf{o})}{\sum_{\mathbf{o} \in \tilde{\mathcal{O}}} p_n(\mathbf{o})} \quad (6)$$

and

$$\begin{aligned} \tilde{g}_{\text{epist}}(\tilde{\mathcal{S}}, \tilde{\mathcal{O}}) &= -\frac{1}{N} \sum_{\mathbf{o} \in \tilde{\mathcal{O}}} \ln \left( \frac{1}{N} \sum_{\mathbf{s} \in \tilde{\mathcal{S}}} p(\mathbf{o}|\mathbf{s}) \right) \\ &\quad - \frac{1}{N} \sum_{\mathbf{s} \in \tilde{\mathcal{S}}} \mathcal{H}(p(\mathbf{o}|\mathbf{s})), \end{aligned} \quad (7)$$

under the assumption that the entropy  $\mathcal{H}(p(\mathbf{o}|\mathbf{s})) : \mathcal{S} \rightarrow \mathbb{R}$  can be calculated analytically. The original model [33] had calculated  $g_{\text{epist}}$  by using KDE methods based on  $\tilde{\mathcal{O}}$  to approximate  $\tilde{q}_o(\mathbf{o}) = \mathbb{E}_{\tilde{q}_s(\mathbf{s})} p(\mathbf{o}|\mathbf{s})$ , compared to us using  $\frac{1}{N} \sum_{\mathbf{s} \in \tilde{\mathcal{S}}} p(\mathbf{o}|\mathbf{s})$ . We opted for this different approach, as the original estimation would result

in an over-approximation of  $\tilde{q}_o(\mathbf{o})$ , given that we evaluate the KDE exclusively at the center of each kernel. Consequently, we use the following approximation  $\tilde{G}$  for the EFE:

$$\begin{aligned}\tilde{G}(\boldsymbol{\pi}_t, q(\mathbf{s}_t)) &= \sum_{\tau=t+1}^{t+H} -\tilde{g}_{\text{pragm}}\left(\tilde{\mathbf{O}}_{\tau}\right) \\ &\quad -\tilde{g}_{\text{epist}}\left(\tilde{\mathbf{S}}_{\tau}, \tilde{\mathbf{O}}_{\tau}\right).\end{aligned}\quad (8)$$

When evaluating the pragmatic value, we assume that the preference (i.e. the distribution of desired observations)  $p(\mathbf{o})$  accounts for four aspects of the agent's objective: a) to maintain its desired longitudinal velocity, b) to minimize the magnitude of control inputs, c) to remain on the road and within its current lane (e.g., avoiding lane markers or opposite lanes), d) prevent collisions, and e) avoiding hazardous situations. Each of these aspects is represented by an individual preference function (Supplementary Materials 1.2.4), which are multiplied together:

$$\begin{aligned}p(\mathbf{o}) &= \mathcal{N}(v_{\text{ego}}|\mu_v, \sigma_v) \mathcal{N}(a_{\text{long,ego}}|0, \sigma_a) \mathcal{N}(\omega_{\text{ego}}|0, \sigma_{\omega}) \\ &\quad p_{\text{plat}}(y_{\text{ego}}) p_{\text{coll}}(\mathbf{o}) p_{\text{safe}}(\mathbf{o}).\end{aligned}\quad (9)$$

For  $p_{\text{safe}}(\mathbf{o})$ , the model specifically seeks to avoid states where, under the assumption that the other vehicle begins braking suddenly with a deceleration of  $a_{\text{OV,min}}$ , the ego vehicle would fail to avoid a collision despite initiating maximum braking after a response time of 1 s.

## Surprise-based re-planning

Our model assumes that on every time step, the agent performs planning incrementally, unless it observes a surprising event, in which case it re-plans the full policy. Practically, on every time step the agent takes the policy chosen in the previous time step, disregards its first action (as it was already executed) and assumes that the remaining actions constitute all but the last actions of the new policy. The above policy selection mechanism is then used to generate the last action of the new policy.

In parallel with incremental policy updates, on every time step the agent accumulates evidence in favor of a full re-plan, using the accumulation rate  $\lambda$ :

$$E_t = E_{t-1} + \lambda \epsilon_t. \quad (10)$$

Here, we follow Engström *et al.* [6] in accumulating *surprise*  $\epsilon \geq 0$ , defined as the *residual information* of the pragmatic value [47]:

$$\epsilon_t = H \max_{\mathbf{o}} \ln p(\mathbf{o}) - \sum_{\tau=t+1}^{t+H} g_{\text{pragm}}(\tilde{q}_o(\mathbf{o}_{\tau}|\boldsymbol{\pi}_t, q(\mathbf{s}_t))). \quad (11)$$

Under this definition, the *surprise* is the difference between the highest pragmatic value possible and the actual pragmatic value of a policy. For instance, if a policy would result in the most preferred observation, the agent would not accumulate any additional evidence. However, if a policy would lead to an undesired (i.e., *a priori* unlikely) observation, much evidence for a re-plan would be gained.

If the accumulated evidence is below the threshold of 1, the model then follows the extended policy. Otherwise, it generates a completely new policy, applying the above policy selection mechanism to every action in the policy.

Finally, after the policy is determined, its first action  $\mathbf{a}_t$  is used to update the state of the actual world. This is done using the state transition function of the *generative process*:

$$\boldsymbol{\eta}_{t+1} \sim \hat{p}(\boldsymbol{\eta}'|\boldsymbol{\eta}_t, \mathbf{a}_t) \quad (12)$$

## Model parameters

Each of the key model mechanisms has a number of parameters associated with it (see Table 1 for an overview of the 26 most essential parameters). For 12 of them, the exact values have been directly adopted from the literature, in particular the original model [33]. Another thirteen model parameters were treated as free parameters, and were manually tuned to qualitatively match the empirical observations. It was not the purpose of this study to obtain the closest possible fit to human data so no exhaustive parameter optimization was performed.

## Metrics

### Front-to-rear scenario

In this scenario, we used the vehicle trajectory and driver input data to extract brake response times and deceleration magnitudes. To that end, we followed Markkula *et al.* [14], extracting response

**Table 1:** An overview of the most essential parameters used in the full model. For tuned parameters, we normally only tested three to four different parameters, with the drift rate  $\lambda$  being the noticeable exception.

Parameter	Description	Source
State transition function $p(\mathbf{s}' \mathbf{s}, \mathbf{a})$		
$\Delta t = 0.2 \text{ s}$	Time step size	Model of routine driving [33]
$4.2 \text{ m} \times 1.72 \text{ m}$	Vehicle size	Matching [56]
$w = 3.65 \text{ m}$	Lane width	Matching [56]
$\sigma_{a,0} = 3 \text{ ms}^{-2}$	Noise applied to other vehicle's acceleration during belief update	Tuned parameter
$\sigma_{\omega,0} = 0.4575 \text{ ms}^{-2}$	Noise applied to other vehicle's steering rate during belief update	Tuned parameter
$\sigma_a = 0.6 \text{ ms}^{-2}$	Noise applied to other vehicle's acceleration during behavior prediction	Tuned parameter
$\sigma_{\omega} = 0.0915 \text{ ms}^{-2}$	Noise applied to other vehicle's steering rate during behavior prediction	Tuned parameter
Observation probability $p(\mathbf{o} \mathbf{s})$		
$\dot{\phi}_0 = 0.00215 \text{ s}^{-1}$	Looming threshold	Taken from [42]
Preference function $p(\mathbf{o})$		
$\mu_v = v_0$	Mean of preference distribution of agent's velocity $v$	Model of routine driving [33]
$\sigma_v = 0.5 \text{ ms}^{-1}$	Standard deviation of preference distribution of agent's velocity $v$	Tuned parameter
$\sigma_a = 0.1 \text{ ms}^{-2}$	Standard deviation of preference distribution of agent's acceleration $a$	Tuned parameter
$\sigma_{\omega} = 0.02 \text{ s}^{-1}$	Standard deviation of preference distribution of agent's steering rate $\omega$	Tuned parameter
$g_{LL} = -15000$	Pragmatic value for leaving the road	Tuned parameter
$g_{LC} = -1000$	Pragmatic value for driving on a lane boundary or in opposing lanes	Tuned parameter
$g_C = -10000$	Pragmatic value after collision with relative velocity of $10 \text{ ms}^{-1}$	Tuned parameter
Policy selection		
$H = 30$	Prediction horizon	Model of routine driving [33]
$N = 75$	Number of particles	Model of routine driving [33]
$K = 10$	Number of iterations of policy sampling	Model of routine driving [33]
$M = 100$	Tuned parameter	
$\beta = 0.1$	$\beta M$ samples with lowest EFE are used as base for next iteration	Model of routine driving [33]
$\mathcal{N}(0, 5 \text{ ms}^{-2})$	Distribution to sample accelerations $a_{\tau}$ in first iteration from	Model of routine driving [33] (mean) and Tuned parameter (std)
$\mathcal{N}(0, 0.1 \text{ s}^{-1})$	Distribution to sample steering rates $\omega_{\tau}$ in first iteration from	Model of routine driving [33] (mean) and Tuned parameter (std)
$a_0 = -0.1 \text{ ms}^{-2}$	Acceleration applied when no pedal is pressed	Logical consideration
$\lambda = 10^{-5.9}$	Evidence accumulation drift rate	Tuned parameter

times by fitting a piecewise-linear function to the recorded velocity data; the brake response time was then determined as the time instant when the first constant line switches to one with falling velocity. The slope of this line was used as the estimated deceleration magnitude.

### Lateral incursion scenario

In this scenario, we extracted brake and steering response times following Johnson et al. [56], by interpolating along the acceleration  $a_{\text{long}}$  and steering angle  $\delta$  data to find the time at which  $-1 \text{ ms}^{-2}$  and  $0.0077 \text{ rad}$  (i.e., a steering wheel angle of  $5^\circ$ ) are exceeded, to extract brake and steering response times respectively.

## Conflict of Interest

JE, MO'K, LJ and JM were employed by Waymo LLC and conducted the research without any external funding from third-parties. Techniques discussed in this paper may be described in U.S. Patent Application Nos. 18/614,428 and 63/657,623. Delft University of Technology received funding from Waymo LLC for parts of the research carried out by JFS, but JFS received no direct financial benefit for his contributions to the paper.

## Acknowledgments

We thank Daphne Cornelisse for creating figures 1 and 2, as well as Martijn Wisse, Todd Hester, and Trent Victor for providing helpful feedback on the manuscript.

## Author contributions

**Julian F. Schumann:** Methodology, Software, Validation, Formal analysis, Investigation, Writing - Original Draft, Visualization. **Johan Engström:** Conceptualization, Validation, Writing - Original Draft, Supervision, Project administration, Funding acquisition. **Leif Johnson:** Formal analysis, Writing - Review & Editing, Visualization. **Matthew O'Kelly:** Writing - Review & Editing. **Joao Messias:** Writing - Review & Editing. **Jens Kober:** Writing - Review & Editing, Supervision. **Arkady Zgonnikov:** Resources,

Writing - Review & Editing, Supervision, Project administration, Funding acquisition.

# 1 Supplementary Material

## 1.1 Active Inference Framework

To model the behavior of human drivers in different scenarios, we combine Active Inference and Evidence Accumulation. For sake of either notation, we use the shorthand of  $\mathbf{b}_{1:B} = \{b_i | i \in \{1, \dots, B\}\}$ . Additionally, while the predicted beliefs about states  $\tilde{q}_s(\mathbf{s}_\tau)$  and observations  $\tilde{q}_o(\mathbf{o}_\tau)$  for  $\tau > t$  depend on the current belief  $q(\mathbf{s}_t)$  and the chosen policy  $\pi_t$  (sequence of planned actions), so that the correct notation would be  $\tilde{q}_s(\mathbf{s}_\tau | \pi_t, q(\mathbf{s}_t))$  and  $\tilde{q}_o(\mathbf{o}_\tau | \pi_t, q(\mathbf{s}_t))$  respectively, we will use the shorthand expressions  $\tilde{q}_s(\mathbf{s}_\tau)$  and  $\tilde{q}_o(\mathbf{o}_\tau)$  to improve readability.

### 1.1.1 Generative process and Generative model

The basic concept of active inference is the idea that a human agent does not know the actual mechanism underlying their surrounding world (called *generative process*), but instead relies on an internal model (the so called *generative model*) approximating the true world. These describe how the true state of the world ( $\eta_t$ ), a state of the agents' belief about the world ( $\mathbf{s}_t$ ), the agent's actions ( $\mathbf{a}_t$ ), and the observations of the true world  $\mathbf{o}_t$  at a time  $t$  interact with each other. Here, the *generative process* consists out of two parts:

- The true transition probability  $\hat{p}(\eta_{t+1} | \eta_t, \mathbf{a}_t)$ . It describes how a certain action at time  $t$  influences the future world state.
- The true observation probability  $\hat{p}(\mathbf{o}_t | \eta_t)$ . It describes how likely it is that a certain observation can be perceived given the current state of the world.

Meanwhile, the *generative model* consists out of two parts as well.

- The internal state transition probability  $p(\mathbf{s}_{t+1} | \mathbf{s}_t, \mathbf{a}_t, \theta_s)$ , which might be parameterized by  $\theta_s$ .
- The internal observation probability  $p(\mathbf{o}_t | \mathbf{s}_t, \theta_o)$ , which might be parameterized by  $\theta_o$ .

The second main idea of active inference is that an agent is uncertain about its belief about the world  $\mathbf{s}_t$ , meaning that instead of a single values, we instead assume that the agent holds a probabilistic belief, denoted by  $q(\mathbf{s}_t)$ . In general, the agent could also have some uncertainty regarding the generative model itself (i.e., there is a probabilistic belief  $q(\theta)$  about the *generative model*'s parameters  $\theta = \{\theta_o, \theta_s\}$ ), but we will not include this assumption in favor of a computationally more efficient model. We represent stochastic beliefs  $q(\mathbf{s}_t)$  by  $N = 75$  equally likely representative samples  $\mathbf{S}_t = \mathbf{s}_{t,1:N}$ .

Given a world with the previous state  $\eta_{t-1}$ , an belief  $\mathbf{S}_{t-1}$ , and a chosen action  $\mathbf{a}_{t-1}$ , we can update those in the following way:

1. We randomly sample our future world state  $\eta_t$  using the transition probability of the *generative process*:

$$\eta_t \sim \hat{p}(\eta' | \eta_{t-1}, \mathbf{a}_{t-1}) \quad (\text{A13})$$

2. We generate the observations  $\mathbf{o}_t$  that the agent makes. Under the assumption that the uncertainties in the *generative process* are negligible compared to the uncertainties in the *generative model*, we use the expected value:

$$\mathbf{o}_t = \mathbb{E}_{\hat{p}(\mathbf{o}' | \eta_t)} \mathbf{o}' \quad (\text{A14})$$

3. We lastly have to update the internal belief of the agent. Here, using variational inference, we get:

$$\begin{aligned} q(\mathbf{s}_t) &\propto p(\mathbf{o}_t | \mathbf{s}_t, \theta_o) \mathbb{E}_{q(\mathbf{s}_{t-1})} p(\mathbf{s}_t | \mathbf{s}_{t-1}, \mathbf{a}_{t-1}, \theta_s) \\ &\propto p(\mathbf{o}_t | \mathbf{s}_t, \theta_o) q_A(\mathbf{s}_t) \end{aligned} \quad (\text{A15})$$

To apply this to our sample based belief representation, we first generate the updated samples  $\mathbf{S}_{A,t} = \mathbf{s}_{A,t,1:N}$  that represent  $q_A(\mathbf{s}_t)$  and follow from the internal state transition probability

$p(\mathbf{s}_t | \mathbf{s}_{t-1}, \mathbf{a}_{t-1}, \boldsymbol{\theta}_s)$ , with  $\mathbf{s}_{A,t,n} \sim p(\mathbf{s}' | \mathbf{s}_{t-1,n}, \mathbf{a}_{t-1}, \boldsymbol{\theta}_s)$ . One can then get an explicit approximation for  $q_A(\mathbf{s}_t)$  using a Kernel Density Estimate (KDE) based on  $\mathbf{S}_{A,t}$ , which can be expressed as

$$q_A(\mathbf{s}_t) \approx \frac{1}{N} \sum_{n=1}^N \mathcal{N}(\mathbf{s}_t | \mathbf{s}_{A,t,n}, \boldsymbol{\Sigma}_{A,t}) . \quad (\text{A16})$$

At this point, with  $q_A$  and  $p(\mathbf{o} | \mathbf{s})$  both known, one could generate the updated belief samples  $\mathbf{S}_t$  with a form of the Metropolis Hastings algorithm, which is however computationally inefficient.

Instead, a faster update is possible, as long as there exists a bijective mapping  $\mathcal{L}$  under which  $p(\mathbf{o} | \mathbf{s})$  can be expressed as a normal distribution:

$$\begin{aligned} p(\mathbf{o}_t | \mathbf{s}_t, \boldsymbol{\theta}_o) &= \mathcal{N}(\mathcal{L}(\mathbf{o}_t) | \mu(\mathcal{L}(\mathbf{o}_t)) + \mathcal{L}(\mathbf{A}\mathbf{s}_t + \mathbf{b}), \boldsymbol{\Sigma}(\mathcal{L}(\mathbf{o}_t))) |\det J_{\mathcal{L}}(\mathbf{o}_t)| \\ &= \mathcal{N}(\mathcal{L}(\mathbf{A}\mathbf{s}_t + \mathbf{b}) | \mathcal{L}(\mathbf{o}_t) - \mu(\mathcal{L}(\mathbf{o}_t)), \boldsymbol{\Sigma}(\mathcal{L}(\mathbf{o}_t))) |\det J_{\mathcal{L}}(\mathbf{o}_t)| \end{aligned} \quad (\text{A17})$$

Then, instead doing our update over  $\mathbf{s}$  directly, we can instead do it over  $\mathbf{s}_{\mathcal{L},t} = \mathcal{L}(\mathbf{A}\mathbf{s}_t + \mathbf{b})$ . Namely, we can use a KDE to instead calculate  $q_{\mathcal{L},A}(\mathbf{s}_{\mathcal{L},t})$ , where with  $\mathbf{s}_{\mathcal{L},A,t,n} = \mathcal{L}(\mathbf{A}\mathbf{s}_{A,t,n} + \mathbf{b})$  we get

$$q_{\mathcal{L},A}(\mathbf{s}_{\mathcal{L},t}) \approx \frac{1}{N} \sum_{n=1}^N \mathcal{N}(\mathbf{s}_{\mathcal{L},t} | \mathbf{s}_{\mathcal{L},A,t,n}, \boldsymbol{\Sigma}_{\mathcal{L},A,t}) . \quad (\text{A18})$$

Substituting (A18) and (A17) then allows us to express  $q_{\mathcal{L}}(\mathbf{s}_{\mathcal{L},t})$  as a Gaussian multi mixture model, from which sampling  $\mathbf{S}_{\mathcal{L},t}$  is trivial:

$$\begin{aligned} q(\mathbf{s}_t) &\propto p(\mathbf{o}_t | \mathbf{s}_t, \boldsymbol{\theta}_o) q_A(\mathbf{s}_t) \\ \iff q_{\mathcal{L}}(\mathbf{s}_{\mathcal{L},t}) &\propto \mathcal{N}(\mathbf{s}_{\mathcal{L},t} | \mathcal{L}(\mathbf{o}_t) - \mu(\mathcal{L}(\mathbf{o}_t)), \boldsymbol{\Sigma}(\mathcal{L}(\mathbf{o}_t))) q_{\mathcal{L},A}(\mathbf{s}_{\mathcal{L},t}) \\ &\propto \sum_{n=1}^N \mathcal{N}(\mathbf{s}_{\mathcal{L},t} | \mathcal{L}(\mathbf{o}_t) - \mu(\mathcal{L}(\mathbf{o}_t)), \boldsymbol{\Sigma}(\mathcal{L}(\mathbf{o}_t))) \mathcal{N}(\mathbf{s}_{\mathcal{L},t} | \mathbf{s}_{\mathcal{L},A,t,n}, \boldsymbol{\Sigma}_{\mathcal{L},A,t}) \\ &\propto \sum_{n=1}^N w_{t,n} \mathcal{N}(\mathbf{s}_{\mathcal{L},t} | \boldsymbol{\mu}_{t,n}, \boldsymbol{\Sigma}_t) \end{aligned} \quad (\text{A19})$$

with  $\boldsymbol{\mu}_o = \mathcal{L}(\mathbf{o}_t) - \mu(\mathcal{L}(\mathbf{o}_t))$

$$\begin{aligned} \boldsymbol{\Sigma}_t &= \left( \boldsymbol{\Sigma}_{\mathcal{L},A,t}^{-1} + \boldsymbol{\Sigma}(\mathcal{L}(\mathbf{o}_t))^{-1} \right)^{-1} \\ \boldsymbol{\mu}_{t,n} &= \boldsymbol{\Sigma}_t \left( \boldsymbol{\Sigma}_{\mathcal{L},A,t}^{-1} \mathbf{s}_{\mathcal{L},A,t,n} + \boldsymbol{\Sigma}(\mathcal{L}(\mathbf{o}_t))^{-1} \boldsymbol{\mu}_o \right) \\ w_{t,n} &\propto \exp \left( \frac{1}{2} (\mathbf{s}_{\mathcal{L},A,t,n} - \boldsymbol{\mu}_o)^T (\boldsymbol{\Sigma}_{\mathcal{L},A,t} + \boldsymbol{\Sigma}(\mathcal{L}(\mathbf{o}_t)))^{-1} (\mathbf{s}_{\mathcal{L},A,t,n} - \boldsymbol{\mu}_o) \right) . \end{aligned} \quad (\text{A20})$$

After sampling  $\mathbf{s}_{\mathcal{L},t,1:N}$  from the GMM, we can get our final sample  $\mathbf{S}_t = \mathbf{s}_{t,1:N}$  with  $\mathbf{s}_{t,n} = \mathbf{A}^{-1}(\mathcal{L}^{-1}(\mathbf{s}_{\mathcal{L},t,n}) - \mathbf{b})$ .

If  $\mathbf{A}$  is not full rank, we will have to simply assume that the distribution  $q(\mathbf{s}_t)$  orthogonally to the image of  $\mathbf{A}$  will be identical to the one in  $q_A(\mathbf{s}_t)$ . However, it must be noted that in our simulations  $\mathbf{A}$  will be the identity matrix.

In the update of our model, we use a time step size of  $\Delta t = 0.2$  s

### 1.1.2 Expected Free Energy

After the agent updates its internal belief  $q(\mathbf{s})$ , it then has to generate a new policy  $\boldsymbol{\pi}_t = \mathbf{a}_{t:(t+H-1)}$  (with  $\mathbf{a}_t = [\pi_t]_1$ ) over a prediction horizon of  $H$  time steps (we use  $H = 30$  in our implementation). In general active inference, it is postulated that such a plan is selected based on the minimization of the *expected free energy*  $G$ , here defined using the preference function  $p(\mathbf{o})$ :

$$\begin{aligned} G(\boldsymbol{\pi}_t | q(\mathbf{s}_t)) &= \sum_{\tau=t+1}^{t+H} g(\boldsymbol{\pi}_t, q(\mathbf{s}_t), \tau) \\ &= \sum_{\tau=t+1}^{t+H} -\underbrace{\mathbb{E}_{\tilde{q}_o(\mathbf{o}_\tau)p_n(\mathbf{o}_\tau)} \ln p(\mathbf{o}_\tau)}_{\text{Pragmatic value } g_{\text{pragm}}} - \underbrace{(\mathcal{H}(\tilde{q}_o(\mathbf{o}_\tau)) - \mathbb{E}_{\tilde{q}_s(\mathbf{s}_\tau)} \mathcal{H}(p(\mathbf{o}_\tau | \mathbf{s}_\tau, \boldsymbol{\theta}_o)))}_{\text{Epistemic value } g_{\text{epist}}} \end{aligned} \quad (\text{A21})$$

Here, the normative probability  $p_n$  is used to implement some norm-conditioned belief about the likelihood of observations (i.e., while some observation  $\mathbf{o}_\tau$  might be kinematically equally likely to others in  $\tilde{\mathcal{O}}_\tau$ , it might be perceived as less likely because it violates some norms, such as driving on the wrong side of the road). We call this use of  $p_n$  a norm-conditioned particle filter. It must be noted that it could be argued that such beliefs are better implemented directly in the state transition function, this would require a much more detailed balancing of  $p_n$ , complicating the fitting of the model. Therefore, for reasons of simplicity, we chose the current approach. Meanwhile,  $\tilde{q}_s(\mathbf{s}_\tau)$  and  $\tilde{q}_o(\mathbf{o}_\tau)$  correspond to the beliefs that the agents predicts for internal states and observations when following a certain policy, with

$$\begin{aligned} \tilde{q}_s(\mathbf{s}_\tau) &= \mathbb{E}_{\tilde{q}_s(\mathbf{s}_{\tau-1})} p(\mathbf{s}_\tau | \mathbf{s}_{\tau-1}, \mathbf{a}_{\tau-1}, \boldsymbol{\theta}_s) \\ \tilde{q}_o(\mathbf{o}_\tau) &= \mathbb{E}_{\tilde{q}_s(\mathbf{s}_\tau)} p(\mathbf{o}_\tau | \mathbf{s}_\tau, \boldsymbol{\theta}_o) \end{aligned} \quad (\text{A22})$$

We use again our sample based approach for belief representation, with  $\tilde{\mathcal{S}}_\tau = \mathbf{s}_{\tau,1:N}$  representing  $\tilde{q}_s(\mathbf{s}_\tau)$  (with  $\mathbf{s}_{\tau,n} \sim p(\mathbf{s}' | \mathbf{s}_{\tau-1,n}, \mathbf{a}_{\tau-1}, \boldsymbol{\theta}_s)$ ) and  $\tilde{\mathcal{O}}_\tau = \mathbf{o}_{\tau,1:N}$  approximating  $\tilde{q}_o(\mathbf{o}_\tau)$  (where  $\mathbf{o}_{\tau,n} \sim p(\mathbf{o}' | \mathbf{s}_{\tau,n}, \boldsymbol{\theta}_o)$ ). For the initial step of  $\tau = t+1$ , we can assume that  $\tilde{\mathcal{S}}_t = \mathcal{S}_t$ . Based on this, one can then calculate the expected free energy  $g$  at one timestep with

$$\begin{aligned} g(\boldsymbol{\pi}_t, q(\mathbf{s}_t), \tau) &\approx - \frac{\sum_{\mathbf{o}_\tau \in \tilde{\mathcal{O}}_\tau} p_n(\mathbf{o}_\tau) \ln p(\mathbf{o}_\tau)}{\sum_{\mathbf{o}_\tau \in \tilde{\mathcal{O}}_\tau} p_n(\mathbf{o}_\tau)} \\ &\quad - \left( \mathcal{H}(\tilde{q}_o(\mathbf{o}_\tau)) - \frac{1}{N} \sum_{\mathbf{s}_\tau \in \tilde{\mathcal{S}}_\tau} \mathcal{H}(p(\mathbf{o}' | \mathbf{s}_\tau, \boldsymbol{\theta}_o)) \right), \end{aligned} \quad (\text{A23})$$

where we use the approximation

$$\begin{aligned} \mathcal{H}(\tilde{q}_o(\mathbf{o}_\tau)) &= \mathcal{H}(\mathbb{E}_{\tilde{q}_s(\mathbf{s}_\tau)} p(\mathbf{o}_\tau | \mathbf{s}_\tau, \boldsymbol{\theta}_o)) \\ &= -\frac{1}{N} \sum_{\mathbf{o}_\tau \in \tilde{\mathcal{O}}_\tau} \ln \left( \frac{1}{N} \sum_{\mathbf{s}_\tau \in \tilde{\mathcal{S}}_\tau} p(\mathbf{o}_\tau | \mathbf{s}_\tau, \boldsymbol{\theta}_o) \right) \end{aligned} \quad (\text{A24})$$

To maximize  $G$ , we use the Cross Entropy Method (CEM) for model predictive control, which is an iterative method over  $k \in 1, \dots, K$  with  $K = 20$ :

1. We define a distribution  $p_{\pi,k}(\boldsymbol{\pi}_t) = \mathcal{N}(\boldsymbol{\pi}_t | \boldsymbol{\mu}_{\pi,t,k-1}, \text{diag}(\boldsymbol{\sigma}_{\pi,t,k-1}^2))$  over the policy space, from which we sample the  $M = 100$  policies  $\boldsymbol{\pi}_{t,k,1:M}$  from  $p_{\pi,k}(\boldsymbol{\pi}_t)$  and calculate the respective expected free energy (after adjusting for pedals with  $f_{\text{real}}$ )  $G_{t,k,m} = G(f_{\text{real}}(\boldsymbol{\pi}_{t,k,m}), q(\mathbf{s}_t))$  (see (A23)).
2. We select the  $\beta = 0.1 \in [0, 1]$  percent samples  $\boldsymbol{\pi}_{t,k,1:M}$  with the lowest expected free energy.
3. We update our distribution, where  $\boldsymbol{\mu}_{\pi,t,k}$  and  $\boldsymbol{\sigma}_{\pi,t,k}$  are the mean and standard deviation of the aforementioned  $\beta M$  selected best plans.

For the first iteration, we choose  $\boldsymbol{\mu}_{\pi,t,0} = \mathbf{0}$ , while we choose as standard deviations in  $\boldsymbol{\sigma}_{\pi,t,0}$  value of  $5 \text{ ms}^{-2}$  for accelerations  $a$  and  $0.1 \text{ s}^{-1}$  for steering rates  $\omega$ . The final policy is then selected as

$$\boldsymbol{\pi}_t = f_{\text{real}} \left( \underset{m \in \{1, \dots, M\}}{\text{argmin}} G(f_{\text{real}}(\boldsymbol{\pi}_{t,K,m}), q(\mathbf{s}_t)) \right). \quad (\text{A25})$$

Here,  $f_{\text{real}}$  is used to prevent unrealistically control inputs.

### 1.1.3 Evidence Accumulation

Commonly, the policy  $\boldsymbol{\pi}_t$  is re-chosen at every timestep. However, research has shown that humans tend to make decisions (such a changing preselected policies) only if there is enough evidence supporting such a decision, in a process called *evidence accumulation*. Here, we implement this concept by having the agent accumulate evidence  $E_t$  towards the need for selecting a new policy. The agent then updates its policy in the following way:

1. We our previous policy  $\boldsymbol{\pi}_{t-1}$ , resulting in  $\tilde{\boldsymbol{\pi}}_t$ , with  $[\tilde{\boldsymbol{\pi}}_t]_{1:H-1} = [\boldsymbol{\pi}_{t-1}]_{2:H}$ , and only optimize the last needed time step  $[\tilde{\boldsymbol{\pi}}_t]_H$  with the method described in 1.1.2.
2. We calculate the evidence for choosing a new plan based on the normalized, negative pragmatic value (i.e., the *surprise*), with

$$\epsilon_t = \epsilon(\tilde{\boldsymbol{\pi}}_t | q(\mathbf{s}_t)) = H \max_{\mathbf{o}'} \ln p(\mathbf{o}') - \sum_{\tau=t+1}^{t+H} \mathbb{E}_{\tilde{q}_o(\mathbf{o}_\tau)} \ln p(\mathbf{o}_\tau, \mathbf{a}_{\tau-1}). \quad (\text{A26})$$

We then update our accumulated surprise with  $E_t = E_{t-1} + \lambda \epsilon_t$ , where we use a drift rate of  $\lambda = 10^{-5.9}$ .  
3. If we see that  $E_t \geq 1$ , then we optimize the full policy  $\boldsymbol{\pi}_t$  using the method described in 1.1.2, and set  $E_t = 0$ . Otherwise, we use the continued policy  $\tilde{\boldsymbol{\pi}}_t$  as our current policy  $\boldsymbol{\pi}_t$

## 1.2 Specific Models

While the previous section described our general framework for using active inference, this section will detail the exact *generative process* and *generative model* we used in our scenarios.

### 1.2.1 State transition probability

When implementing the model, we use for the state transition function of both the *generative process* and the *generative model* a common bicycle model  $B$ . In this, model each vehicle can be defined by three parameters, its width  $d$ , its front length  $l_f$  and its rear length  $l_r$ . Additionally, the kinematic state of each agent then consists of its position markers  $x$  and  $y$ , its longitudinal speed  $v$ , its current heading angle  $\theta$  and steering angle  $\delta$  ( $\mathbf{x} = \{x, y, v, \theta, \delta\}$ ). Each agent is then controlled by the acceleration  $a_{\text{long}} \in [-a_{\text{max}}, a_{\text{max}}]$  and steering rate  $\omega \in [-\omega_{\text{max}}, \omega_{\text{max}}]$  with  $a_{\text{max}} = 8 \text{ ms}^{-2}$  and  $\omega_{\text{max}} = 1.22 \text{ s}^{-1}$

( $\mathbf{u} = \{a_{\text{long}}, \omega\}$ ). One then can get the differential equation  $\dot{\mathbf{x}} = B(\mathbf{x}, \mathbf{u})$ :

$$\begin{aligned}\dot{x} &= v \cos(\theta + \beta) \\ \dot{y} &= v \sin(\theta + \beta) \\ \dot{v} &= k_{\text{tire}} a_{\text{long}} \\ \dot{\theta} &= \frac{v}{l_f + l_r} \tan(k_{\text{tire}} \delta) \cos(\beta) \\ \dot{\delta} &= \begin{cases} 0 & \frac{\text{sgn}(\omega)\text{sgn}(\delta)}{k_{\text{tire}}} > 1 \\ \omega & \text{Otherwise} \end{cases} \\ \text{with } \beta &= \arctan\left(\frac{l_r}{l_f + l_r} \tan(k_{\text{tire}} \delta)\right)\end{aligned}\tag{A27}$$

Here, we use  $k_{\text{tire}}$  and  $\hat{\delta}$  to represent the limitations imposed by the tire friction:

$$k_{\text{tire}} = \frac{a_{\text{max}}}{\max \left\{ a_{\text{max}}, \sqrt{a_{[\text{long}]}^2 + \left(\frac{v^2}{l_f + l_r} \delta\right)^2} \right\}}\tag{A28}$$

In each scenario, where we model the ego agent in interaction with the other agents  $V = \{V_1, V_2, \dots\}$ , we then can generally find the control actions  $\mathbf{a} = \mathbf{u}_{\text{ego}}$  and  $\boldsymbol{\eta} = \mathbf{o} = \mathbf{s} = \{\mathbf{x}_\nu, \mathbf{u}_\nu | \nu \in \{\text{ego}\} \cup V\}$ . We assume that the *generative process* is deterministic, which allows us to get the following, where  $f_B(\mathbf{x}, \mathbf{u})$  describes the usage of Heun's methods to propagate the state forward according to equation (A27):

$$\begin{aligned}\hat{p}(\boldsymbol{\eta}' | \boldsymbol{\eta}, \mathbf{a}) &= \delta(\mathbf{x}'_{\text{ego}} - f_B(\mathbf{x}_{\text{ego}}, \mathbf{a})) \delta(\mathbf{u}'_{\text{ego}} - \mathbf{a}) \\ &\quad \prod_{\nu \in V} \delta(\mathbf{x}'_\nu - f_B(\mathbf{x}_\nu, \mathbf{u}_\nu)) \delta(\mathbf{u}'_\nu - \mathbf{u}_{\nu, \text{preset}})\end{aligned}\tag{A29}$$

Here, the next control inputs  $\mathbf{u}_{\nu, \text{preset}}$  are predefined to allow the other vehicle to follow a prescribed trajectory, which depends on the scenario (see 1.3.1 and 1.3.2). Meanwhile, some uncertainty is involved in the *generative model*:

$$\begin{aligned}p(\mathbf{s}' | \mathbf{s}, \mathbf{a}, \boldsymbol{\theta}_s) &= \delta(\mathbf{x}'_{\text{ego}} - f_B(\mathbf{x}_{\text{ego}}, \mathbf{a})) \delta(\mathbf{u}'_{\text{ego}} - \mathbf{a}) \\ &\quad \prod_{\nu \in V} \delta(\mathbf{x}'_\nu - f_B(\mathbf{x}_\nu, \mathbf{u}_\nu)) \mathcal{N}(\mathbf{u}'_\nu | \mathbf{u}_\nu, \text{diag}(\boldsymbol{\sigma}_\mathbf{u}^2))\end{aligned}\tag{A30}$$

In our model, we assume  $\boldsymbol{\sigma}_\mathbf{u} = \boldsymbol{\sigma}_{\mathbf{u}, 0} = [3 \text{ ms}^{-2}, 0.4575 \text{ s}^{-1}]$  when updating our belief (see (A15)) and

$$\boldsymbol{\sigma}_\mathbf{u} = 0.2 f_v(\mathbb{E}_{\tilde{q}_o(\mathbf{o})} p_n(\mathbf{o})) \boldsymbol{\sigma}_{\mathbf{u}, 0}\tag{A31}$$

when predicting future states during model evaluation (see (A22)). Here,  $p_n$  is the weighting used in equation (A23), with

$$f_v(p) = \frac{1}{2 \max \{ \min \{p, 0.505\}, 0.01 \} - 0.01} : [0, 1] \rightarrow [1, 10]\tag{A32}$$

being used to give the agent less certainty in its belief about the future state of the other vehicle if its current state violates traffic norms.

### 1.2.2 Observation probability

For the *generative process*, we assume that observations are exact.

$$\hat{p}(\mathbf{o}'|\boldsymbol{\eta}) = \delta(\mathbf{o}' - \boldsymbol{\eta}) \quad (\text{A33})$$

For the *generative model* meanwhile, we use a observation probability that follows the style laid out in equation (A17). Here, we implement the looming based perception using the bijective mapping  $\{\mathbf{x}_{\text{ego}}, \boldsymbol{\varphi}\} = \mathcal{L}(\mathbf{x}_{\text{ego}}, \mathbf{x}_{\text{OV}}, \mathbf{u}_{\text{OV}}|\mathbf{a})$  with  $\boldsymbol{\varphi} = \{\varphi, \dot{\varphi}, \ddot{\varphi}, y_{\text{OV}}, \theta_{\text{OV}}, \delta_{\text{OV}}, \omega_{\text{OV}}\}$ , where looming angle  $\varphi$ , looming  $\dot{\varphi}$ , and looming rate  $\ddot{\varphi}$  are calculated as:

$$\begin{aligned} \varphi &\approx 2 \arctan \left( \frac{d}{2(x_{\text{OV}} - x_{\text{ego}})} \right) \\ \dot{\varphi} &\approx -\frac{d(v_{\text{OV}} \cos(\theta_{\text{OV}}) - v_{\text{ego}})}{(x_{\text{OV}} - x_{\text{ego}})^2 + \frac{1}{4}d^2} \\ \ddot{\varphi} &\approx \frac{d}{(x_{\text{OV}} - x_{\text{ego}})^2 + \frac{1}{4}d^2} \left( a_{\text{long,ego}} - a_{\text{OV}} \cos(\theta_{\text{OV}}) + \frac{2(x_{\text{OV}} - x_{\text{ego}})(v_{\text{OV}} \cos(\theta_{\text{OV}}) - v_{\text{ego}})^2}{(x_{\text{OV}} - x_{\text{ego}})^2 + \frac{1}{4}d^2} \right). \end{aligned} \quad (\text{A34})$$

It must be noted that this mapping is a rough one-dimensional estimate assuming that  $\theta_{\text{ego}} \approx 0$ . However, looming based perception update is the only used if the other agent is roughly in front of it, as it unreasonable to assume that the ego vehicle would perceive the other vehicle directly with their eyes if it is not in front of them. So technically, we find that:

if in the actual world state  $\boldsymbol{\eta}$  where

$$\mathcal{L}(\mathbf{o}|\mathbf{a}) = \mathcal{L}(\mathbf{x}_{\text{ego}}, \mathbf{x}_{\text{OV}}, \mathbf{u}_{\text{OV}}|\mathbf{a}) = \begin{cases} \{\mathbf{x}_{\text{ego}}, \boldsymbol{\varphi}\} & x_{\text{OV}} - x_{\text{ego}} > l_r + l_f \\ \mathbf{x}_{\text{ego}}, \mathbf{x}_{\text{OV}}, \mathbf{u}_{\text{OV}} & \text{Otherwise} \end{cases} \quad (\text{A35})$$

As our state and observation states  $\mathbf{s}$  and  $\mathbf{o}$  overlap, in Equation (A17), we use  $\mathbf{A} = \mathbf{I}$  and  $\mathbf{b} = \mathbf{0}$ . we also have to implement the looming threshold, for which we use the function  $\mu(\mathbf{o}_{\mathcal{L}})$ . Given a looming threshold of  $\dot{\varphi}_0 = 0.00215 \text{ s}^{-1}$ , we can define here:

$$\mu(\mathbf{o}_{\mathcal{L}}) = \begin{cases} \mu_{\text{loom}}(\mathbf{o}_{\mathcal{L}}) & (x_{\text{OV}} - x_{\text{ego}} > l_r + l_f) \wedge (|\dot{\varphi}| \leq \dot{\varphi}_0) \\ \mathbf{0} & \text{Otherwise} \end{cases} \quad (\text{A36})$$

with

$$\mu_{\text{loom}}(\mathbf{o}_{\mathcal{L}}) = \begin{Bmatrix} 0 \\ 0 \\ 0 \\ 0 \\ 0 \\ 0 \\ \dot{\varphi} \\ \ddot{\varphi} - \frac{d}{(x_{\text{OV}} - x_{\text{ego}})^2 + \frac{1}{4}d^2} a_{\text{ego}} \\ 0 \\ 0 \\ 0 \\ 0 \end{Bmatrix}^T. \quad (\text{A37})$$

Meanwhile, we also have to define the function  $\Sigma(\mathbf{o}_L) = \text{diag}(\boldsymbol{\sigma}(\mathbf{o}_L)^2)$ , where

$$\boldsymbol{\sigma}(\mathbf{o}_L) = \{\boldsymbol{\sigma}_{\text{ego}}, \boldsymbol{\sigma}_{\text{OV}}(\mathbf{o}_L)\} \quad (\text{A38})$$

with

$$\boldsymbol{\sigma}_{\text{ego}} = \{0.0002 \text{ m}, 0.000001 \text{ m}, 0.0002 \text{ ms}^{-1}, 0.000001, 0.000001\} \quad (\text{A39})$$

and

$$\boldsymbol{\sigma}_{\text{OV}}(\mathbf{o}_L) = \begin{cases} \left\{ \begin{array}{c} 0.0002 \text{ m} \\ 0.00002 \text{ m} \\ 0.0002 \text{ ms}^{-1} \\ 0.0002 \\ 0.002 \\ 0.00002 \text{ ms}^{-2} \\ 0.002 \text{ s}^{-1} \end{array} \right\}^T & x_{\text{OV}} - x_{\text{ego}} < l_r + l_f \\ \left\{ \begin{array}{c} 0.00001 \\ 0.00001 \text{ s}^{-1} \\ 0.000001 \text{ s}^{-2} \\ 0.00002 \text{ m} \\ 0.0002 \\ 0.002 \\ 0.002 \text{ s}^{-1} \end{array} \right\}^T & (x_{\text{OV}} - x_{\text{ego}} > l_r + l_f) \wedge (|\dot{\varphi}| > \dot{\varphi}_0) \\ \left\{ \begin{array}{c} 0.00001 \\ 0.0043 \text{ s}^{-1} \\ 0.00043 \text{ s}^{-2} \\ 0.00002 \text{ m} \\ 0.0002 \\ 0.002 \\ 0.002 \text{ s}^{-1} \end{array} \right\}^T & (x_{\text{OV}} - x_{\text{ego}} > l_r + l_f) \wedge (|\dot{\varphi}| \leq \dot{\varphi}_0) \end{cases} \quad (\text{A40})$$

### 1.2.3 Control limits

We also want to limit the acceleration and deceleration patterns not achievable by actual human input. To this end, we use  $f_{\text{real}}$  (equation (A25)), which in our case will use two functions,  $f_{\text{pedal}}$  and  $f_{\text{jerk}}$ .  $f_{\text{pedal}}$  prevents unrealistically fast switching between gas and brake pedals, by setting for an acceleration  $a_{\text{long},\tau}$ :

$$f_{\text{pedal}}(a_{\text{long},\tau}) = \begin{cases} a_0 & (a_{\text{long},\tau-1} - a_0)(a_{\text{long},\tau} - a_0) < 0 \\ a_\tau & \text{otherwise} \end{cases} \quad (\text{A41})$$

It must be noted that in our current model we assume that the acceleration observed when releasing both pedals is  $a_0 = -0.1 \text{ ms}^{-2}$ , to approximate the fact that with neutral pedals, wind and roll resistances will lead to some decelerations.

Meanwhile,  $f_{\text{jerk}}$  tries to implement realistic speeds at which the pedals can be pressed and released, by limiting the jerks applied:

$$f_{\text{jerk}}(a_{\text{long},\tau}) = \min \{a_{\text{long},\tau-1} + j_{\min} \Delta t, \max \{a_{\text{long},\tau}, a_{\text{long},\tau-1} + j_{\max} \Delta t\}\} \quad (\text{A42})$$

For the jerk limits, we use:

$$j_{\min} = \begin{cases} -5 \text{ ms}^{-3} & (a_{\text{long},\tau-1} - a_{\text{long},\tau-2}) < 0 \wedge (a_{\text{long},\tau} - a_{\text{long},\tau-1}) > 0 \\ -30 \text{ ms}^{-3} & \text{otherwise} \end{cases} \quad (\text{A43})$$

$$j_{\max} = \begin{cases} 0 \text{ ms}^{-3} & (a_{\text{long},\tau-1} - a_{\text{long},\tau-2}) > 0 \wedge (a_{\text{long},\tau} - a_{\text{long},\tau-1}) < 0 \\ \begin{cases} 5 \text{ ms}^{-3} & a_{\text{long},\tau} \geq 0 \\ 15 \text{ ms}^{-3} & a_{\text{long},\tau} < 0 \end{cases} & \text{otherwise} \end{cases}$$

Both those functions are applied recursively, with

$$[f_{\text{real}}(\boldsymbol{\pi})]_{\tau} = f_{\text{pedal}}(f_{\text{jerk}}(f_{\text{pedal}}([f_{\text{real}}(\boldsymbol{\pi})]_{\tau-1}))) \quad (\text{A44})$$

#### 1.2.4 Preference function

We use the following preference function  $p$  when minimizing the expected free energy  $G$  (see (A23)):

$$p(\boldsymbol{o}) = \mathcal{N}(v_{\text{ego}}|v_0, \sigma_v) \mathcal{N}(a_{\text{long,ego}}|0, \sigma_a) \mathcal{N}(\omega_{\text{ego}}|0, \sigma_{\omega}) p_{\text{lat}}(y_{\text{ego}}) p_{\text{coll}}(\boldsymbol{o}) p_{\text{safe}}(\boldsymbol{o}) \quad (\text{A45})$$

Here,

$$p_{\text{lat}}(y_{\text{ego}}) = \mathcal{T}\left(y_{\text{rel}}(y_{\text{ego}}) \mid \frac{w-d}{2}, g_{LC}, g_{LL}\right) \quad (\text{A46})$$

with the triangular function  $\mathcal{T}$ :

$$\mathcal{T}(x|x_0, p_1, p_2) \propto \begin{cases} \exp\left(\frac{|x|}{x_0} p_1\right) & |x| \leq x_0 \\ \exp(p_2) & \text{otherwise} \end{cases} \quad (\text{A47})$$

We also need to define the collision preference  $p_{\text{coll}}$ :

$$p_{\text{coll}}(\boldsymbol{o}_{\tau}) = \min\{p_{\text{coll}}(\boldsymbol{o}_{\tau-1}), f_{\text{coll}}(\boldsymbol{o}_{\tau})\} \quad (\text{A48})$$

This minimum is here so that all timesteps following upon a collision are still punished, as the model itself has no collision mechanics, allowing vehicles to phase through each other. We then get the collision preference at a single timestep  $f_{\text{coll}}$ , where we have collision condition  $\mathcal{C}(\boldsymbol{o}) = |y_{\text{OV}} - y_{\text{ego}}| \leq 1.15 d \wedge |x_{\text{OV}} - x_{\text{ego}}| \leq 1.15 (l_f + l_r)$ :

$$f_{\text{coll}}(\boldsymbol{o}) = \begin{cases} \exp\left(g_C \left(0.2 + 0.8 \frac{v_{\text{ego}} - v_{\text{OV}} \cos(\theta_{\text{ego}} - \theta_{\text{OV}})}{10 \text{ ms}^{-1}}\right)\right) & \mathcal{C}(\boldsymbol{o}) \\ \begin{cases} 1 & x_{\text{OV}} - x_{\text{ego}} \leq l_r + l_f \\ \mathcal{N}\left(\frac{\dot{\varphi}}{\varphi} \mid 0.2 \text{ s}^{-1}, \sigma_{\tau^{-1}}\right) & \text{Otherwise} \end{cases} & \text{Otherwise} \end{cases} \quad (\text{A49})$$

Here, the mean for the normal distribution over  $\tau^{-1} = \frac{\dot{\varphi}}{\varphi}$  is taken from Markkula *et al.* [14]. In the collision cases ( $\mathcal{C}(\boldsymbol{o})$ ), we adjust the collision cost based on the collision speed, as it is likely that human agents prefer to collide with lower impact velocities, if a collision cannot be avoided.

Lastly, we define  $p_{\text{safe}}$ , where we mainly consider the feasibility of braking when in a car following scenario:

$$p_{\text{safe}}(\boldsymbol{o}_{\tau}) = \begin{cases} \exp\left(\frac{1}{2} g_C \left(0.2 + 0.8 \frac{v_{\text{ego}} - v_{\text{OV}} \cos(\theta_{\text{ego}} - \theta_{\text{OV}})}{10 \text{ ms}^{-1}}\right)\right) & \mathcal{C}_{\text{brake}}(\boldsymbol{o}) \wedge a_{\text{ego, req}} < -a_{\max} \\ 1 & \text{Otherwise} \end{cases} \quad (\text{A50})$$

Here, the condition  $\mathcal{C}_{\text{brake}}$  for being in a car following scenario is defined as:

$$\mathcal{C}_{\text{brake}}(\mathbf{o}) = (|y_{\text{OV}} - y_{\text{ego}}| \leq 1.15 d) \wedge (x_{\text{OV}} - x_{\text{ego}} \geq (l_f + l_r)) \wedge (\text{sgn}(v_{\text{ego}}) \text{sgn}(v_{\text{OV}} \cos(\theta_{\text{OV}})) \geq 0) \quad (\text{A51})$$

Meanwhile,  $a_{\text{ego, req}}$  is the required deceleration applied after a reaction time of  $t_{\text{react}}$  needed to avoid a collision if the other vehicle suddenly started to accelerate towards/brake in front of the ego vehicle with  $a_{\text{OV,test}} = \min\{a_{\text{long,OV}}, a_{\text{OV,min}}\}$ .

$$\begin{aligned} a_{\text{ego, req}} &= -\frac{1}{2} \frac{\max\{v_{\text{ego,react}}, 0\}^2}{\max\{d_{\text{ego,react}} - 1.15(l_f + l_r), 0\}} \\ v_{\text{ego,react}} &= v_{\text{ego}} + \min\{a_{\text{long,ego}}, 0\} t_{\text{react}} \\ d_{\text{ego,react}} &= \left( x_{\text{OV}} - \frac{1}{2} \frac{v_{\text{OV}}^2}{a_{\text{OV,test}}} \right) - \left( x_{\text{ego}} + v_{\text{ego}} t_{\text{react}} + \frac{1}{2} \min\{a_{\text{long,ego}}, 0\} t_{\text{react}}^2 \right) \end{aligned} \quad (\text{A52})$$

The preference function can then be parameterized by the eight parameters  $\sigma_v = 0.5 \text{ ms}^{-1}$ ,  $\sigma_a = 0.1 \text{ ms}^{-2}$ ,  $\sigma_\omega = 0.02 \text{ s}^{-1}$ ,  $\sigma_{\tau^{-1}} = 0.125 \text{ s}^{-1}$ ,  $g_{LC} = -1000$ ,  $g_{LL} = -5000$ ,  $g_C = -10000$ ,  $t_{\text{react}} = 1 \text{ s}$ . Meanwhile, depending on the simulation, we choose  $a_{\text{OV,min}}$  so that the given initial distance and speed would result in stable car following, with lower bound of  $a_{\text{min}} = -a_{\text{max}} = -8 \text{ ms}^{-2}$ . Specifically, we simulate a one-lane front-to-rear scenario with a leading other vehicle at constant velocity  $v_0$  for multiple values of  $a_{\text{OV,min}}$ . For each simulation, we then extract the steady-state following distance that the agent chose for following, and the corresponding time gap. When given a velocity  $v_0$  and desired following distance or desired time gap, we use linear interpolation to extract the corresponding value of  $a_{\text{OV,min}}$  from the given data points.

While our framework is aimed to be as generalizable as possible, there are still some changes in between our two models. Namely, when calculating the  $y_{\text{rel}}$  from equation (A52), we have to represent that in the front-to-rear scenario both lanes go in one direction, while in the lateral incursion scenario, the left lane is designed for oncoming traffic.

### 1.3 Specific scenarios

#### 1.3.1 Front-to-rear scenario

The first scenario, which models the response of a driver to the leading other vehicle suddenly braking, contains two vehicles ( $V = \{\text{ego, OV}\}$ ).

##### Initial state

In this scenario, there are 12 initial conditions, with  $\mathbf{x}_{\text{ego,0}} = \{0 \text{ m}, 0 \text{ m}, v_0, 0, 0\}$  and  $\mathbf{x}_{\text{OV,0}} = \{v_0 \Delta t_{\text{tgp,0}} + l_f + l_r, 0 \text{ m}, v_0, 0, 0\}$ , with  $\Delta t_{\text{tgp,0}} \in \{0.5 \text{ s}, 1.0 \text{ s}, 1.5 \text{ s}, 2.0 \text{ s}, 2.5 \text{ s}, 3.0 \text{ s}, 3.5 \text{ s}\}$  and  $v_0 \in \{10 \text{ ms}^{-1}, 15 \text{ ms}^{-1}, 25 \text{ ms}^{-1}, 35 \text{ ms}^{-1}\}$ . Meanwhile, we assume a lane width  $w = 3.65 \text{ m}$ , and vehicle sizes of  $d = 1.72 \text{ m}$ ,  $l_f = 2.1 \text{ m}$ , and  $l_r = 2.1 \text{ m}$ .

##### Other vehicles behavior

In this scenario, we set  $\mathbf{u}_{\text{OV,preset}}$  so that the other vehicle will drive straight on for exactly 5 s, after which it will start to decelerate, applying a jerk of  $-10 \text{ ms}^{-3}$  until reaching an acceleration value of  $-6 \text{ ms}^{-2}$ . It will keep this acceleration until it comes to a standstill.

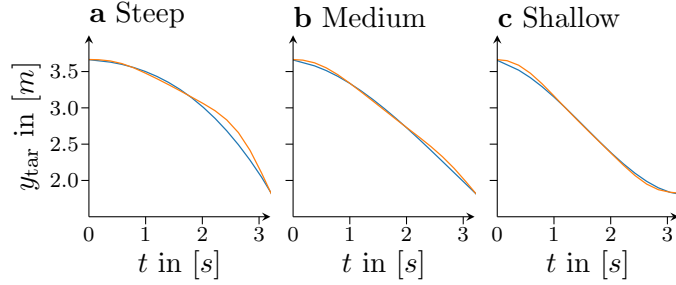


**Fig. A1:** The different maneuvers by the other vehicle. The orange line represents the trajectory used in our simulation, while the blue line corresponds to the original experiment [56].  $t = 0$  corresponds to the start of the maneuver, while the horizontal velocity stays constant. Afterwards, the model continues along a straight line with constant velocity.

### Lateral preference

Here, we calculate the lateral relative position  $y_{\text{rel}}$  from equation (A52) as:

$$y_{\text{rel}}(y_{\text{ego}}) = \begin{cases} y_{\text{ego}} & y_{\text{ego}} \leq \frac{w-d}{2} \\ \frac{w-d}{2} & \frac{w-d}{2} < y_{\text{ego}} \leq \frac{w+d}{2} \\ y_{\text{ego}} - w & \frac{w+d}{2} < y_{\text{ego}} \end{cases} \quad (\text{A53})$$

### Norm conditioning

We define the normative probability  $p_n(o)$  (see (A23)) in the following way, that punishes moving into the left lane ( $p = 0.02$ ) or leaving the road ( $p = 0.01$ ) :

$$p_n(o) = \begin{cases} 1 & -\frac{w-d}{2} \leq y_{\text{OV}} \leq \frac{w-d}{2} \\ 0.02 & \frac{w-d}{2} \leq y_{\text{OV}} < \frac{3w-d}{2} \\ 0.01 & \text{Otherwise} \end{cases} \quad (\text{A54})$$

Given the usage of  $p_n(o)$  as a weighing function, it is excusable to not normalize it here.

### 1.3.2 Lateral incursion scenario

The second scenario also only contains out of two vehicles ( $V = \{\text{ego}, \text{OV}\}$ ).

#### Initial state

In this scenario, there is a single initial condition, with  $\mathbf{x}_{\text{ego},0} = \{0 \text{m}, 0 \text{m}, v_0, 0, 0\}$  and  $\mathbf{x}_{\text{OV},0} = \{300 \text{m}, 0 \text{m}, v_0, \pi, 0\}$  (the initial velocities  $v_0 = 17.88 \text{ ms}^{-1}$  correspond to 40 mph). Lane width and vehicle size are identical to the front-to-rear scenario (see 1.3.1)

#### Other vehicle's behavior

The other vehicle's path is preprogrammed in a manner that it starts turning to the left when the time to collision  $((x_{\text{OV}} - x_{\text{ego}})/(v_{\text{OV}} + v_{\text{ego}}))$  falls below 5.15 s. This turn will last for 3.3 s, at which point the other vehicle's front left corner should start crossing the central lane marker, after which the other vehicle will follow a straight path. Following [56], we run this scenario in 3 different variants, where after 5.15 s seconds, we perceive  $y_{\text{OV}} = -0.4w$  (Steep incursion),  $y_{\text{OV}} = 0 \text{ m}$  (Medium incursion), or  $y_{\text{OV}} = 0.45w$  (Shallow incursion) (see Figure A1).

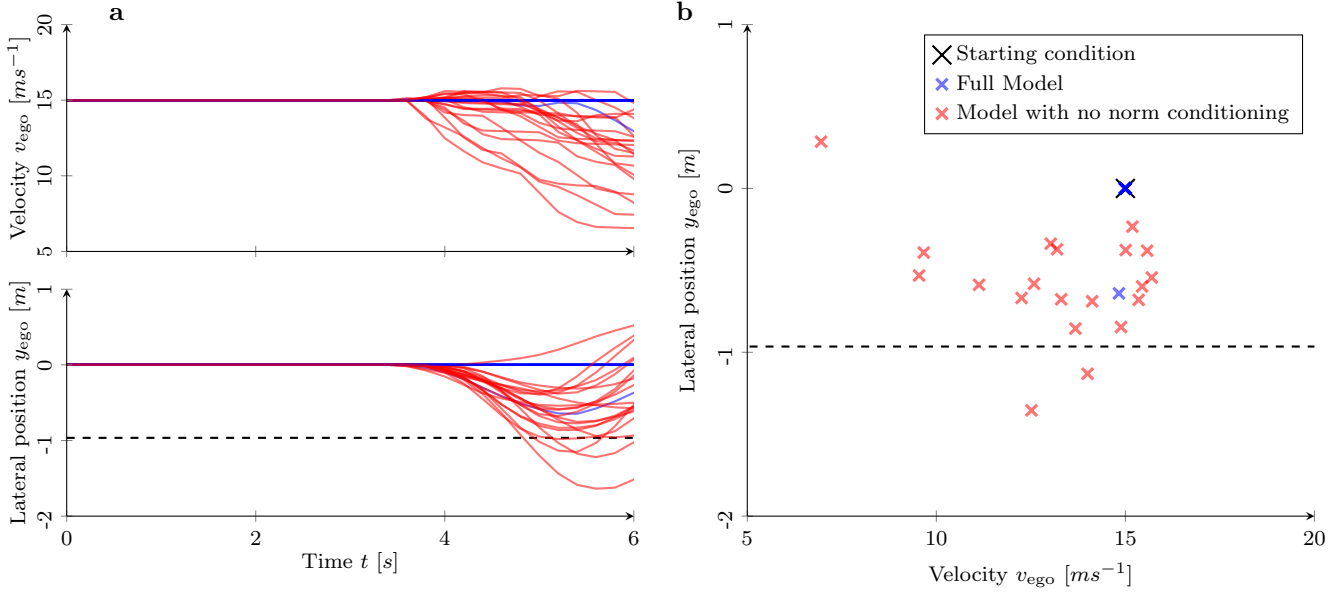


**Fig. A2:** Results in the 20 repetitions of the non-incursion scenario, for both the model with norm conditioned particle filter (blue) and without (red). **a**) Change of longitudinal velocity  $v_{\text{ego}}$  and lateral position  $y_{\text{ego}}$  of simulated agents over time. **b**) The kinematic state of the ego vehicle at the point in time when passing the oncoming other vehicle.

#### Lateral preference

Here, we calculate the lateral relative position  $y_{\text{rel}}$  from equation (A52) as:

$$y_{\text{rel}}(y_{\text{ego}}) = \begin{cases} y_{\text{ego}} & y_{\text{ego}} \leq \frac{w-d}{2} \\ \frac{w-d}{2} & \frac{w-d}{2} < y_{\text{ego}} \leq \frac{3w-d}{2} \\ y_{\text{ego}} - w & \frac{3w-d}{2} < y_{\text{ego}} \end{cases} \quad (\text{A55})$$

#### Norm conditioning

We define the normative probability  $p_n(\mathbf{o})$  (see (A23)) in the following way, that punishes moving into the opposite lane ( $p = 0.02$ ), and punishes leaving the road even more ( $p = 0.01$ ) :

$$p_n(\mathbf{o}) = \begin{cases} 1 & \frac{w+d}{2} \leq y_{\text{OV}} \leq \frac{3w-d}{2} \\ 0.02 & -\frac{w-d}{2} \leq y_{\text{OV}} < \frac{w+d}{2} \\ 0.01 & \text{Otherwise} \end{cases} \quad (\text{A56})$$

Given the usage of  $p_n(\mathbf{o})$  as a weighing function, it is excusable to not normalize it here.

#### 1.4 Benign scenario

This is a variation of the lateral incursion scenario, where the other vehicle just drives along its lane without any change in direction or speed. Specifically, we start the vehicles at an initial distance of 150 m, both driving with  $15 \text{ ms}^{-1}$ . Those simulations are repeated 20 times for both the full proposed model as well as the one without the norm conditioned particle filter. As seen in Figure A2, the full model – with one very jumpy exception – does not deviate from its desired state in response to the other agent. This is much different in the model without norm conditioning, where the vehicles either move to the right,

or brake, or do both. With such behavior not very realistic in everyday driving scenarios, those results highlight the need for the norm-conditioned particle filter. Of course, it must be noted that similar results without the norm-conditioned particle filter could be achieved by simply removing the prediction noise, but it was shown in the main text that that is essential for realistic collision avoidance behavior.

## References

- [1] J. Bärgman, V. Lisovskaja, T. Victor, C. Flannagan, M. Dozza, How does glance behavior influence crash and injury risk? A ‘what-if’ counterfactual simulation using crashes and near-crashes from SHRP2. *Transportation Research Part F: Traffic Psychology and Behaviour* **35**, 152–169 (2015). <https://doi.org/10.1016/j.trf.2015.10.011>. URL <https://www.sciencedirect.com/science/article/pii/S136984781500162X>
- [2] J. Engström, G. Markkula, Q. Xue, N. Merat, Simulating the effect of cognitive load on braking responses in lead vehicle braking scenarios. *IET Intelligent Transport Systems* **12**(6), 427–433 (2018). <https://doi.org/10.1049/iet-its.2017.0233>. URL <https://onlinelibrary.wiley.com/doi/abs/10.1049/iet-its.2017.0233>. eprint: <https://onlinelibrary.wiley.com/doi/pdf/10.1049/iet-its.2017.0233>
- [3] G. Bianchi Piccinini, E. Lehtonen, F. Forcolin, J. Engström, D. Albers, G. Markkula, J. Lodon, J. Sandin, How Do Drivers Respond to Silent Automation Failures? Driving Simulator Study and Comparison of Computational Driver Braking Models. *Human Factors: The Journal of the Human Factors and Ergonomics Society* **62**(7), 1212–1229 (2020). <https://doi.org/10.1177/0018720819875347>. URL <http://journals.sagepub.com/doi/10.1177/0018720819875347>
- [4] N. Montali, J. Lambert, P. Mougin, A. Kuefler, N. Rhinehart, M. Li, C. Gulino, T. Emrich, Z. Yang, S. Whiteson, B. White, D. Anguelov, The Waymo Open Sim Agents Challenge. *Advances in Neural Information Processing Systems* **36**, 59151–59171 (2023). URL [https://proceedings.neurips.cc/paper\\_files/paper/2023/hash/b96ce67b2f2d45e4ab315e13a6b5b9c5-Abstract-Datasets\\_and\\_Benchmarks.html](https://proceedings.neurips.cc/paper_files/paper/2023/hash/b96ce67b2f2d45e4ab315e13a6b5b9c5-Abstract-Datasets_and_Benchmarks.html)
- [5] P. Olleja, G. Markkula, J. Bärgman. Validation of human benchmark models for Automated Driving System approval: How competent and careful are they really? (2024). <https://doi.org/10.48550/arXiv.2406.09493>. URL <http://arxiv.org/abs/2406.09493>. ArXiv:2406.09493
- [6] J. Engström, S.Y. Liu, A. Dinparastdjadid, C. Simoiu, Modeling road user response timing in naturalistic traffic conflicts: A surprise-based framework. *Accident Analysis & Prevention* **198**, 107460 (2024). <https://doi.org/10.1016/j.aap.2024.107460>. URL <https://www.sciencedirect.com/science/article/pii/S0001457524000058>
- [7] P.J. Matusz, S. Dikker, A.G. Huth, C. Perrodin, Are We Ready for Real-world Neuroscience? *Journal of Cognitive Neuroscience* **31**(3), 327–338 (2019). [https://doi.org/10.1162/jocn\\_e\\_01276](https://doi.org/10.1162/jocn_e_01276). URL [https://doi.org/10.1162/jocn\\_e\\_01276](https://doi.org/10.1162/jocn_e_01276)
- [8] S.G. Shamay-Tsoory, A. Mendelsohn, Real-Life Neuroscience: An Ecological Approach to Brain and Behavior Research. *Perspectives on Psychological Science* **14**(5), 841–859 (2019). <https://doi.org/10.1177/1745691619856350>. URL <https://doi.org/10.1177/1745691619856350>. Publisher: SAGE Publications Inc
- [9] W. Carvalho, A. Lampinen. Naturalistic Computational Cognitive Science: Towards generalizable models and theories that capture the full range of natural behavior (2025). <https://doi.org/10.48550/arXiv.2502.20349>. URL <http://arxiv.org/abs/2502.20349>. ArXiv:2502.20349 [q-bio]
- [10] Q. Xue, G. Markkula, X. Yan, N. Merat, Using perceptual cues for brake response to a lead vehicle: Comparing threshold and accumulator models of visual looming. *Accident Analysis & Prevention* **118**, 114–124 (2018). <https://doi.org/10.1016/j.aap.2018.06.006>. URL <https://linkinghub.elsevier.com/retrieve/pii/S0001457518302239>

[11] M. Svärd, G. Markkula, J. Bärgman, T. Victor, Computational modeling of driver pre-crash brake response, with and without off-road glances: Parameterization using real-world crashes and near-crashes. *Accident Analysis & Prevention* **163**, 106433 (2021). <https://doi.org/10.1016/j.aap.2021.106433>. URL <https://www.sciencedirect.com/science/article/pii/S0001457521004644>

[12] C. Guo, X. Wang, L. Su, Y. Wang, Safety distance model for longitudinal collision avoidance of logistics vehicles considering slope and road adhesion coefficient. *Proceedings of the Institution of Mechanical Engineers* (2021). URL <https://journals.sagepub.com/doi/full/10.1177/0954407020959744>

[13] O. Siebinga, A. Zgonnikov, D.A. Abbink, A model of dyadic merging interactions explains human drivers' behavior from control inputs to decisions. *PNAS Nexus* **3**(10), pgae420 (2024). <https://doi.org/10.1093/pnasnexus/pgae420>. URL <https://doi.org/10.1093/pnasnexus/pgae420>

[14] G. Markkula, J. Engström, J. Lodin, J. Bärgman, T. Victor, A farewell to brake reaction times? Kinematics-dependent brake response in naturalistic rear-end emergencies. *Accident Analysis & Prevention* **95**, 209–226 (2016). <https://doi.org/10.1016/j.aap.2016.07.007>. URL <https://www.sciencedirect.com/science/article/pii/S0001457516302366>

[15] R. Wei, A.D. McDonald, A. Garcia, H. Alambeigi, Modeling Driver Responses to Automation Failures With Active Inference. *IEEE Transactions on Intelligent Transportation Systems* **23**(10), 18064–18075 (2022). <https://doi.org/10.1109/TITS.2022.3155381>. URL <https://ieeexplore.ieee.org/abstract/document/9733256>. Conference Name: IEEE Transactions on Intelligent Transportation Systems

[16] T. Li, J. Kovaceva, M. Dozza, Modeling collision avoidance maneuvers for micromobility vehicles. *Journal of Safety Research* **87**, 232–243 (2023). <https://doi.org/10.1016/j.jsr.2023.09.019>. URL <https://www.sciencedirect.com/science/article/pii/S0022437523001500>

[17] Y. Yuan, X. Weng, Y. Ou, K.M. Kitani, *AgentFormer: Agent-Aware Transformers for Socio-Temporal Multi-Agent Forecasting*, in *IEEE/CVF International Conference on Computer Vision* (2021), pp. 9813–9823

[18] S. Suo, S. Regalado, S. Casas, R. Urtasun, *Trafficsim: Learning to simulate realistic multi-agent behaviors*, in *Proceedings of the IEEE/CVF Conference on Computer Vision and Pattern Recognition* (2021), pp. 10400–10409

[19] T. Gu, G. Chen, J. Li, C. Lin, Y. Rao, J. Zhou, J. Lu, *Stochastic Trajectory Prediction via Motion Indeterminacy Diffusion*, in *Proceedings of the IEEE/CVF Conference on Computer Vision and Pattern Recognition* (2022), pp. 17113–17122. URL [https://openaccess.thecvf.com/content/CVPR2022/html/Gu\\_Stochastic\\_Trajectory\\_Prediction\\_via\\_Motion\\_Indeterminacy\\_Diffusion\\_CVPR\\_2022\\_paper.html](https://openaccess.thecvf.com/content/CVPR2022/html/Gu_Stochastic_Trajectory_Prediction_via_Motion_Indeterminacy_Diffusion_CVPR_2022_paper.html)

[20] M. Igl, D. Kim, A. Kuefler, P. Mougin, P. Shah, K. Shiarlis, D. Anguelov, M. Palatucci, B. White, S. Whiteson, *Symphony: Learning realistic and diverse agents for autonomous driving simulation*, in *2022 International Conference on Robotics and Automation (ICRA)* (IEEE, 2022), pp. 2445–2451

[21] A. Mészáros, J.F. Schumann, J. Alonso-Mora, A. Zgonnikov, J. Kober, *TrajFlow: Learning Distributions over Trajectories for Human Behavior Prediction*, in *2024 IEEE Intelligent Vehicles Symposium (IV)* (Jeju, 2024)

[22] B. Ivanovic, G. Song, I. Gilitschenski, M. Pavone, trajdata: A Unified Interface to Multiple Human Trajectory Datasets. Advances in Neural Information Processing Systems **36**, 27582–27593 (2023). URL [https://proceedings.neurips.cc/paper\\_files/paper/2023/hash/57bb67dbe17bfb660c8c63d089ea05b9-Abstract-Datasets\\_and\\_Benchmarks.html](https://proceedings.neurips.cc/paper_files/paper/2023/hash/57bb67dbe17bfb660c8c63d089ea05b9-Abstract-Datasets_and_Benchmarks.html)

[23] J.F. Schumann, J. Kober, A. Zgonnikov, Benchmarking Behavior Prediction Models in Gap Acceptance Scenarios. IEEE Transactions on Intelligent Vehicles **8**(3), 2580–2591 (2023). <https://doi.org/10.1109/TIV.2023.3244280>

[24] K. Friston, T. FitzGerald, F. Rigoli, P. Schwartenbeck, G. Pezzulo, Active Inference: A Process Theory. Neural Computation **29**(1), 1–49 (2017). [https://doi.org/10.1162/NECO\\_a\\_00912](https://doi.org/10.1162/NECO_a_00912). URL [https://doi.org/10.1162/NECO\\_a\\_00912](https://doi.org/10.1162/NECO_a_00912)

[25] L. Da Costa, T. Parr, N. Sajid, S. Veselic, V. Neacsu, K. Friston, Active inference on discrete state-spaces: a synthesis. Journal of Mathematical Psychology **99**, 102447 (2020). <https://doi.org/10.1016/j.jmp.2020.102447>. URL <http://arxiv.org/abs/2001.07203>. ArXiv:2001.07203 [q-bio]

[26] T. Parr, G. Pezzulo, K.J. Friston, *Active Inference: The Free Energy Principle in Mind, Brain, and Behavior* (MIT Press, 2022). Google-Books-ID: UrZNEAAAQBAJ

[27] R. Smith, P. Badcock, K.J. Friston, Recent advances in the application of predictive coding and active inference models within clinical neuroscience. Psychiatry and Clinical Neurosciences **75**(1), 3–13 (2021). <https://doi.org/10.1111/pcn.13138>. URL <https://onlinelibrary.wiley.com/doi/abs/10.1111/pcn.13138>. eprint: <https://onlinelibrary.wiley.com/doi/pdf/10.1111/pcn.13138>

[28] J. Vasil, P.B. Badcock, A. Constant, K. Friston, M.J.D. Ramstead, A World Unto Itself: Human Communication as Active Inference. Frontiers in Psychology **11** (2020). <https://doi.org/10.3389/fpsyg.2020.00417>. URL <https://www.frontiersin.org/journals/psychology/articles/10.3389/fpsyg.2020.00417/full>. Publisher: Frontiers

[29] H. Bottemanne, K.J. Friston, An active inference account of protective behaviours during the COVID-19 pandemic. Cognitive, Affective, & Behavioral Neuroscience **21**(6), 1117–1129 (2021). <https://doi.org/10.3758/s13415-021-00947-0>. URL <https://doi.org/10.3758/s13415-021-00947-0>

[30] D.J. Harris, T. Arthur, D.P. Broadbent, M.R. Wilson, S.J. Vine, O.R. Runswick, An Active Inference Account of Skilled Anticipation in Sport: Using Computational Models to Formalise Theory and Generate New Hypotheses. Sports Medicine **52**(9), 2023–2038 (2022). <https://doi.org/10.1007/s40279-022-01689-w>. URL <https://doi.org/10.1007/s40279-022-01689-w>

[31] F. Novický, A.A. Meera, F. Zeldenrust, P. Lanillos. Precision not prediction: Body-ownership illusion as a consequence of online precision adaptation under Bayesian inference (2024). <https://doi.org/10.1101/2024.09.04.611162>. URL <http://biorxiv.org/lookup/doi/10.1101/2024.09.04.611162>

[32] R. Wei, A. Garcia, A. McDonald, G. Markkula, J. Engström, I. Supeene, M. O’Kelly, *World Model Learning from Demonstrations with Active Inference: Application to Driving Behavior*, in *Active Inference*, ed. by C.L. Buckley, D. Cialfi, P. Lanillos, M. Ramstead, N. Sajid, H. Shimazaki, T. Verbelen (Springer Nature Switzerland, Cham, 2023), Communications in Computer and Information Science, pp. 130–142. [https://doi.org/10.1007/978-3-031-28719-0\\_9](https://doi.org/10.1007/978-3-031-28719-0_9)

[33] J. Engström, R. Wei, A.D. McDonald, A. Garcia, Matthew O’Kelly, L. Johnson, Resolving uncertainty on the fly: modeling adaptive driving behavior as active inference. Frontiers in Neurorobotics **18** (2024). <https://doi.org/10.3389/fnbot.2024.1341750>. URL <https://www.frontiersin.org/articles/10.3389/fnbot.2024.1341750>

- [34] D.N. Lee, A theory of visual control of braking based on information about time-to-collision. *Perception* **5**(4), 437–459 (1976). <https://doi.org/10.1068/p050437>
- [35] J.J. Gibson, *The Ecological Approach to Visual Perception: Classic Edition* (Psychology Press, New York, 2014). <https://doi.org/10.4324/9781315740218>
- [36] R.D. Luce, *Response times: Their role in inferring elementary mental organization* (Oxford University Press on Demand, 1986). Issue: 8
- [37] J.I. Gold, M.N. Shadlen, The neural basis of decision making. *Annu. Rev. Neurosci.* **30**(1), 535–574 (2007)
- [38] R. Ratcliff, H.P. Van Dongen, Diffusion model for one-choice reaction-time tasks and the cognitive effects of sleep deprivation. *Proceedings of the National Academy of Sciences* **108**(27), 11285–11290 (2011)
- [39] G. Markkula, *Modeling driver control behavior in both routine and near-accident driving*, in *Proceedings of the human factors and ergonomics society annual meeting*, vol. 58 (SAGE Publications Sage CA: Los Angeles, CA, 2014), pp. 879–883
- [40] J. Pekkanen, O. Lappi, P. Rinkkala, S. Tuhkanen, R. Frantsi, H. Summala, A computational model for driver's cognitive state, visual perception and intermittent attention in a distracted car following task. *Royal Society Open Science* **5**(9), 180194 (2018). <https://doi.org/10.1098/rsos.180194>. URL <https://royalsocietypublishing.org/doi/full/10.1098/rsos.180194>. Publisher: Royal Society
- [41] E.R. Hoffmann, Estimation of Time to Vehicle Arrival—Effects of Age on Use of Available Visual Information. *Perception* **23**(8), 947–955 (1994). <https://doi.org/10.1068/p230947>. URL <https://doi.org/10.1068/p230947>. Publisher: SAGE Publications Ltd STM
- [42] D. Lamble, M. Laakso, H. Summala, Detection thresholds in car following situations and peripheral vision: implications for positioning of visually demanding in-car displays. *Ergonomics* **42**(6), 807–815 (1999). <https://doi.org/10.1080/001401399185306>. URL <https://doi.org/10.1080/001401399185306>. Publisher: Taylor & Francis eprint: <https://doi.org/10.1080/001401399185306>
- [43] K.P. Murphy, *Machine learning: a probabilistic perspective* (MIT press, 2012)
- [44] H. Laurent, M. Sangnier, C. Treibich, Traffic safety and norms of compliance with rules: An exploratory study. *Economics Bulletin* **41**(4), 2464–2483 (2021). URL <http://www.scopus.com/inward/record.url?scp=85125263034&partnerID=8YFLogxK>
- [45] S. Abbas, S. Fatima, A. Sharif, S.M. Adnan, Drivers' knowledge, attitude and practices towards traffic rules and regulations. *Journal of Road Safety* **35**(3), 24–31 (2024)
- [46] C. Tennant, C. Neels, G. Parkhurst, P. Jones, S. Mirza, J. Stilgoe, Code, culture, and concrete: Self-driving vehicles and the rules of the road. *Frontiers in Sustainable Cities* **3**, 710478 (2021)
- [47] A. Dinparastdjadid, I. Supeene, J. Engstrom, Measuring Surprise in the Wild (2023). <https://doi.org/10.48550/arXiv.2305.07733>. URL <http://arxiv.org/abs/2305.07733>. ArXiv:2305.07733 [cs]
- [48] P.T. de Boer, D.P. Kroese, S. Mannor, R.Y. Rubinstein, A Tutorial on the Cross-Entropy Method. *Annals of Operations Research* **134**(1), 19–67 (2005). <https://doi.org/10.1007/s10479-005-5724-z>.

URL <https://doi.org/10.1007/s10479-005-5724-z>

- [49] H.A. Simon, A behavioral model of rational choice. *The quarterly journal of economics* pp. 99–118 (1955)
- [50] H. Summala, in *Modelling Driver Behaviour in Automotive Environments: Critical Issues in Driver Interactions with Intelligent Transport Systems*, ed. by P.C. Cacciabue (Springer, London, 2007), pp. 189–207. [https://doi.org/10.1007/978-1-84628-618-6\\_11](https://doi.org/10.1007/978-1-84628-618-6_11). URL [https://doi.org/10.1007/978-1-84628-618-6\\_11](https://doi.org/10.1007/978-1-84628-618-6_11)
- [51] H. Oh, J.M. Beck, P. Zhu, M.A. Sommer, S. Ferrari, T. Egner, Satisficing in split-second decision making is characterized by strategic cue discounting. *Journal of Experimental Psychology: Learning, Memory, and Cognition* **42**(12), 1937–1956 (2016). <https://doi.org/10.1037/xlm0000284>. Place: US Publisher: American Psychological Association
- [52] F. Callaway, B. van Opheusden, S. Gul, P. Das, P.M. Krueger, T.L. Griffiths, F. Lieder, Rational use of cognitive resources in human planning. *Nature Human Behaviour* **6**(8), 1112–1125 (2022). <https://doi.org/10.1038/s41562-022-01332-8>
- [53] J. Engstroem, *Scenario criticality determines the effect of working memory load on brake response time*, in *Proceedings of the European Conference on Human Centred Design for Intelligent Transport Systems* (2010), pp. 25–36. URL <https://trid.trb.org/View/1150568>
- [54] K.A. Brookhuis, G. de Vries, D. de Waard, The effects of mobile telephoning on driving performance. *Accident Analysis & Prevention* **23**(4), 309–316 (1991). [https://doi.org/10.1016/0001-4575\(91\)90008-S](https://doi.org/10.1016/0001-4575(91)90008-S). URL <https://www.sciencedirect.com/science/article/pii/000145759190008S>
- [55] J.D. Lee, B. Caven, S. Haake, T.L. Brown, Speech-based interaction with in-vehicle computers: the effect of speech-based e-mail on drivers' attention to the roadway. *Human Factors* **43**(4), 631–640 (2001). <https://doi.org/10.1518/001872001775870340>
- [56] L. Johnson, J. Engström, A. Srinivasan, I. Özturk, G. Markkula, *Looking for an out: Affordances, uncertainty and collision avoidance behavior of human drivers* (2025). URL <https://arxiv.org/abs/2505.14842>
- [57] M. Brännström, E. Coelingh, J. Sjöberg, Decision-making on when to brake and when to steer to avoid a collision. *International Journal of Vehicle Safety* **7**(1), 87–106 (2014). <https://doi.org/10.1504/IJVS.2014.058243>. URL <https://www.inderscienceonline.com/doi/full/10.1504/IJVS.2014.058243>. Publisher: Inderscience Publishers
- [58] V. Venkatraman, J.D. Lee, C.W. Schwarz, Steer or Brake?: Modeling Drivers' Collision-Avoidance Behavior by Using Perceptual Cues. *Transportation Research Record* **2602**(1), 97–103 (2016). <https://doi.org/10.3141/2602-12>. URL <https://doi.org/10.3141/2602-12>. Publisher: SAGE Publications Inc
- [59] M. Hu, Y. Liao, W. Wang, G. Li, B. Cheng, F. Chen, Decision Tree-Based Maneuver Prediction for Driver Rear-End Risk-Avoidance Behaviors in Cut-In Scenarios. *Journal of Advanced Transportation* **2017**, e7170358 (2017). <https://doi.org/10.1155/2017/7170358>. URL <https://www.hindawi.com/journals/jat/2017/7170358/>. Publisher: Hindawi
- [60] A. Sarkar, J.S. Hickman, A.D. McDonald, W. Huang, T. Vogelpohl, G. Markkula, Steering or braking avoidance response in SHRP2 rear-end crashes and near-crashes: A decision tree approach. *Accident Analysis & Prevention* **154**, 106055 (2021). <https://doi.org/10.1016/j.aap.2021.106055>. URL <https://doi.org/10.1016/j.aap.2021.106055>

//www.sciencedirect.com/science/article/pii/S0001457521000865

- [61] M.L. Aust, J. Engström, M. Viström, Effects of forward collision warning and repeated event exposure on emergency braking. *Transportation Research Part F: Traffic Psychology and Behaviour* **18**, 34–46 (2013). <https://doi.org/10.1016/j.trf.2012.12.010>. URL <https://www.sciencedirect.com/science/article/pii/S1369847813000065>
- [62] A.D. McDonald, H. Alambeigi, J. Engström, G. Markkula, T. Vogelpohl, J. Dunne, N. Yuma, Toward Computational Simulations of Behavior During Automated Driving Takeovers: A Review of the Empirical and Modeling Literatures. *Human Factors* **61**(4), 642–688 (2019). <https://doi.org/10.1177/0018720819829572>. URL <https://doi.org/10.1177/0018720819829572>. Publisher: SAGE Publications Inc
- [63] K.D. Kusano, H.C. Gabler, Safety Benefits of Forward Collision Warning, Brake Assist, and Autonomous Braking Systems in Rear-End Collisions. *IEEE Transactions on Intelligent Transportation Systems* **13**(4), 1546–1555 (2012). <https://doi.org/10.1109/TITS.2012.2191542>. URL <https://ieeexplore.ieee.org/abstract/document/6180219>. Conference Name: IEEE Transactions on Intelligent Transportation Systems
- [64] M. Svärd, G. Markkula, J. Engström, F. Granum, J. Bärgman, *A quantitative driver model of pre-crash brake onset and control*, in *Proceedings of the Human Factors and Ergonomics Society Annual Meeting*, vol. 61 (2017), pp. 339–343. <https://doi.org/10.1177/1541931213601565>. URL <https://cir.nii.ac.jp/crid/1360294647862811264>. Publisher: SAGE Publications
- [65] A. Fries, F. Fahrenkrog, K. Donauer, M. Mai, F. Raisch, *Driver behavior model for the safety assessment of automated driving*, in *2022 IEEE Intelligent Vehicles Symposium (IV)* (IEEE, 2022), pp. 1669–1674
- [66] A. Fries, L. Lemberg, F. Fahrenkrog, M. Mai, A. Das, Modeling driver behavior in critical traffic scenarios for the safety assessment of automated driving. *Traffic Injury Prevention* **24**(sup1), S105–S110 (2023). <https://doi.org/10.1080/15389588.2023.2211187>. URL <https://doi.org/10.1080/15389588.2023.2211187>. Publisher: Taylor & Francis .eprint: <https://doi.org/10.1080/15389588.2023.2211187>
- [67] L.F.A. de Oliveira, L. Schories, L. Brostek, M. Meywerk, *Simulation-Based Evaluation of a Generic Autonomous Emergency Braking System Using a Cognitive Pedestrian Behavior Model*, in *27th International Technical Conference on the Enhanced Safety of Vehicles (ESV)* (2023). URL <https://trid.trb.org/View/2211669>. Number: 23-0217
- [68] C. Rössert, J. Drever, L. Brostek. Cognitive behavior model replicates road user response timing in naturalistic rear-end traffic conflicts (2024). <https://doi.org/10.31219/osf.io/su5kt>. URL <https://osf.io/su5kt>
- [69] C. Hubmann, M. Becker, D. Althoff, D. Lenz, C. Stiller, *Decision making for autonomous driving considering interaction and uncertain prediction of surrounding vehicles*, in *2017 IEEE intelligent vehicles symposium (IV)* (IEEE, 2017), pp. 1671–1678
- [70] S. Brechtel, T. Gindele, R. Dillmann, *Probabilistic decision-making under uncertainty for autonomous driving using continuous POMDPs*, in *17th International IEEE Conference on Intelligent Transportation Systems (ITSC)* (2014), pp. 392–399. <https://doi.org/10.1109/ITSC.2014.6957722>
- [71] M. Bouton, A. Cosgun, M.J. Kochenderfer, *Belief state planning for autonomously navigating urban intersections*, in *2017 IEEE Intelligent Vehicles Symposium (IV)* (IEEE, 2017), pp. 825–830

[72] J. Pekkanen, O.T. Giles, Y.M. Lee, R. Madigan, T. Daimon, N. Merat, G. Markkula, Variable-Drift Diffusion Models of Pedestrian Road-Crossing Decisions. *Computational Brain & Behavior* **5**(1), 60–80 (2022). <https://doi.org/10.1007/s42113-021-00116-z>

[73] A. Zgonnikov, D. Abbink, G. Markkula, Should I Stay or Should I Go? Cognitive Modeling of Left-Turn Gap Acceptance Decisions in Human Drivers. *Human Factors* p. 00187208221144561 (2022). <https://doi.org/10.1177/00187208221144561>. URL <https://doi.org/10.1177/00187208221144561>. Publisher: SAGE Publications Inc

[74] J.F. Schumann, A.R. Srinivasan, J. Kober, G. Markkula, A. Zgonnikov, *Using Models Based on Cognitive Theory to Predict Human Behavior in Traffic: A Case Study*, in *2023 IEEE 26th International Conference on Intelligent Transportation Systems (ITSC)* (2023), pp. 5870–5875. <https://doi.org/10.1109/ITSC57777.2023.10421837>. URL <https://ieeexplore.ieee.org/abstract/document/10421837>. ISSN: 2153-0017

[75] T.H.B. FitzGerald, P. Schwartenbeck, M. Moutoussis, R.J. Dolan, K. Friston, Active Inference, Evidence Accumulation, and the Urn Task. *Neural Computation* **27**(2), 306–328 (2015). [https://doi.org/10.1162/NECO\\_a\\_00699](https://doi.org/10.1162/NECO_a_00699). URL [https://doi.org/10.1162/NECO\\_a\\_00699](https://doi.org/10.1162/NECO_a_00699)

[76] F.J. Varela, E. Thompson, E. Rosch, *The embodied mind, revised edition: Cognitive science and human experience* (MIT press, 2017)

[77] E. Thompson, *Mind in life: Biology, phenomenology, and the sciences of mind* (Harvard University Press, 2010)

[78] K. Friston, Life as we know it. *Journal of The Royal Society Interface* **10**(86), 20130475 (2013). <https://doi.org/10.1098/rsif.2013.0475>. URL <https://royalsocietypublishing.org/doi/full/10.1098/rsif.2013.0475>. Publisher: Royal Society

[79] E.D. Paolo, E. Thompson, R. Beer, Laying down a forking path: Tensions between enaction and the free energy principle. *Philosophy and the Mind Sciences* **3** (2022). <https://doi.org/10.3373/phimisci.2022.9187>. URL <https://philosophymindscience.org/index.php/phimisci/article/view/9187>

[80] J. Kiverstein, M.D. Kirchhoff, T. Froese, The Problem of Meaning: The Free Energy Principle and Artificial Agency. *Frontiers in Neurorobotics* **16** (2022). <https://doi.org/10.3389/fnbot.2022.844773>. URL <https://www.frontiersin.org/journals/neurorobotics/articles/10.3389/fnbot.2022.844773/full>. Publisher: Frontiers

[81] K. Friston, in *Affordances in Everyday Life: A Multidisciplinary Collection of Essays*, ed. by Z. Djebbara (Springer International Publishing, Cham, 2022), pp. 211–219. [https://doi.org/10.1007/978-3-031-08629-8\\_20](https://doi.org/10.1007/978-3-031-08629-8_20). URL [https://doi.org/10.1007/978-3-031-08629-8\\_20](https://doi.org/10.1007/978-3-031-08629-8_20)

[82] M.J.D. Ramstead, in *Affordances in Everyday Life: A Multidisciplinary Collection of Essays*, ed. by Z. Djebbara (Springer International Publishing, Cham, 2022), pp. 193–202. [https://doi.org/10.1007/978-3-031-08629-8\\_18](https://doi.org/10.1007/978-3-031-08629-8_18). URL [https://doi.org/10.1007/978-3-031-08629-8\\_18](https://doi.org/10.1007/978-3-031-08629-8_18)

[83] P. Calvo, K. Friston, Predicting green: really radical (plant) predictive processing. *Journal of The Royal Society Interface* **14**(131), 20170096 (2017). <https://doi.org/10.1098/rsif.2017.0096>. URL <https://royalsocietypublishing.org/doi/10.1098/rsif.2017.0096>. Publisher: Royal Society

[84] T. Van de Maele, B. Dhoedt, T. Verbelen, G. Pezzulo, A hierarchical active inference model of spatial alternation tasks and the hippocampal-prefrontal circuit. *Nature Communications* **15**(1), 9892 (2024). <https://doi.org/10.1038/s41467-024-54257-3>. URL <https://www.nature.com/articles/s41467-024-54257-3>

s41467-024-54257-3. Publisher: Nature Publishing Group

- [85] N. Kastel, C. Hesp, K.R. Ridderinkhof, K.J. Friston, Small steps for mankind: Modeling the emergence of cumulative culture from joint active inference communication. *Frontiers in Neurorobotics* **16** (2023). <https://doi.org/10.3389/fnbot.2022.944986>. URL <https://www.frontiersin.org/journals/neurorobotics/articles/10.3389/fnbot.2022.944986/full>. Publisher: Frontiers
- [86] R. Wei, A.D. McDonald, A. Garcia, G. Markkula, J. Engstrom, M. O'Kelly. An active inference model of car following: Advantages and applications (2023). <https://doi.org/10.48550/arXiv.2303.15201>. URL <http://arxiv.org/abs/2303.15201>. ArXiv:2303.15201 [cs]
- [87] K. Friston, L. Da Costa, D. Hafner, C. Hesp, T. Parr, Sophisticated inference. *Neural Computation* **33**(3), 713–763 (2021)
- [88] A. Chohan, G.J. Savelsbergh, P. Van Kampen, M. Wind, M.H. Verheul, Postural adjustments and bearing angle use in interceptive actions. *Experimental brain research* **171**, 47–55 (2006)
- [89] R. Wei, J. Lee, S. Wakayama, A. Tschantz, C. Heins, C. Buckley, J. Carenbauer, H. Thiruvengada, M. Albarracin, M.d. Prado, P. Horling, P. Winzell, R. Rajagopal. Navigation under uncertainty: Trajectory prediction and occlusion reasoning with switching dynamical systems (2024). <https://doi.org/10.48550/arXiv.2410.10653>. URL <http://arxiv.org/abs/2410.10653>. ArXiv:2410.10653
- [90] T. Salzmann, B. Ivanovic, P. Chakravarty, M. Pavone, *Trajectron++: Dynamically-Feasible Trajectory Forecasting with Heterogeneous Data*, in *Computer Vision – ECCV 2020* (Cham, 2020), pp. 683–700. [https://doi.org/10.1007/978-3-030-58523-5\\_40](https://doi.org/10.1007/978-3-030-58523-5_40)
- [91] K. Mangalam, Y. An, H. Girase, J. Malik, *From Goals, Waypoints & Paths to Long Term Human Trajectory Forecasting*, in *Proceedings of the IEEE/CVF International Conference on Computer Vision* (2021), pp. 15233–15242. URL [https://openaccess.thecvf.com/content/ICCV2021/html/Mangalam\\_From\\_Goals\\_Waypoints\\_Paths\\_to\\_Long\\_Term\\_Human\\_Trajectory\\_ICCV\\_2021\\_paper.html](https://openaccess.thecvf.com/content/ICCV2021/html/Mangalam_From_Goals_Waypoints_Paths_to_Long_Term_Human_Trajectory_ICCV_2021_paper.html)
- [92] R. Girgis, F. Golemo, F. Codevilla, M. Weiss, J.A. D'Souza, S.E. Kahou, F. Heide, C. Pal, *LATENT VARIABLE SEQUENTIAL SET TRANSFORMERS FOR JOINT MULTI-AGENT MOTION PREDICTION*, in *10th International Conference on Learning Representations, ICLR 2022* (2022). URL <https://collaborate.princeton.edu/en/publications/latent-variable-sequential-set-transformers-for-joint-multi-agent>
- [93] S. Shi, L. Jiang, D. Dai, B. Schiele, Motion Transformer with Global Intention Localization and Local Movement Refinement. *Advances in Neural Information Processing Systems* **35**, 6531–6543 (2022). URL [https://proceedings.neurips.cc/paper\\_files/paper/2022/hash/2ab47c960bfee4f86dfc362f26ad066a-Abstract-Conference.html](https://proceedings.neurips.cc/paper_files/paper/2022/hash/2ab47c960bfee4f86dfc362f26ad066a-Abstract-Conference.html)
- [94] N. Nayakanti, R. Al-Rfou, A. Zhou, K. Goel, K.S. Refaat, B. Sapp, *Wayformer: Motion Forecasting via Simple & Efficient Attention Networks*, in *2023 IEEE International Conference on Robotics and Automation (ICRA)* (2023), pp. 2980–2987. <https://doi.org/10.1109/ICRA48891.2023.10160609>. URL <https://ieeexplore.ieee.org/abstract/document/10160609>
- [95] P. Lanillos, C. Meo, C. Pezzato, A.A. Meera, M. Baioumy, W. Ohata, A. Tschantz, B. Millidge, M. Wisse, C.L. Buckley, J. Tani. Active Inference in Robotics and Artificial Agents: Survey and Challenges (2021). <https://doi.org/10.48550/arXiv.2112.01871>. URL <http://arxiv.org/abs/2112.01871>. ArXiv:2112.01871 [cs]

[96] P. Mazzaglia, T. Verbelen, O. Çatal, B. Dhoedt, The Free Energy Principle for Perception and Action: A Deep Learning Perspective. *Entropy* **24**(2), 301 (2022). <https://doi.org/10.3390/e24020301>. URL <https://www.mdpi.com/1099-4300/24/2/301>. Number: 2 Publisher: Multidisciplinary Digital Publishing Institute

[97] M.P. Deisenroth, A.A. Faisal, C.S. Ong, *Mathematics for Machine Learning* (Cambridge University Press, 2020). Google-Books-ID: pFjPDwAAQBAJ

[98] J. Fischer, O.S. Tas, *Information Particle Filter Tree: An Online Algorithm for POMDPs with Belief-Based Rewards on Continuous Domains*, in *Proceedings of the 37th International Conference on Machine Learning* (PMLR, 2020), pp. 3177–3187. URL <https://proceedings.mlr.press/v119/fischer20a.html>. ISSN: 2640-3498

[99] P. Polack, F. Altché, B. d'Andréa Novel, A. de La Fortelle, *The kinematic bicycle model: A consistent model for planning feasible trajectories for autonomous vehicles?*, in *2017 IEEE Intelligent Vehicles Symposium (IV)* (2017), pp. 812–818. <https://doi.org/10.1109/IVS.2017.7995816>. URL <https://ieeexplore.ieee.org/abstract/document/7995816>